Quasisynchronization of Reaction–Diffusion Neural Networks Under Deception Attacks

Ruimei Zhang, Hongxia Wang, *Member, IEEE*, Ju H. Park, *Senior Member, IEEE*, Hak-Keung Lam, *Fellow, IEEE*, and Peisong He

***Abstract*—This study focuses on the quasisynchronization problem for reaction–diffusion neural networks (RDNNs) in the presence of deception attacks. Under deception attacks, a time–space sampled-data (TSSD) control mechanism is proposed for RDNNs. Compared with traditional control strategies, the proposed control mechanism can not only save network bandwidth but also improve the cybersecurity of communications. Inspired by Halanay's inequality, a new inequality is proposed, which can be effectively applied to the quasisynchronization problem for dynamical systems. Then, by using this inequality and the Lyapunov functional approach, quasisynchronization criteria are set for RDNNs. The desired control gain is gained from solving a group of linear matrix inequalities. Moreover, in the absence of deception attacks, the exponential synchronization problem is studied for RDNNs. In the end, simulation results are given to demonstrate the usefulness of the theoretical analysis.**

***Index Terms*—Deception attacks, quasisynchronization, reaction–diffusion neural networks (RDNNs), time–space sampled-data (TSSD) control.**

I. Introduction

OVER the past decades, neural networks have attracted increasing attention because of their extensive applications in several areas, such as model identification, stock market prediction, cryptography, and combinatorial optimization [1]–[6]. Great efforts heretofore have been devoted to investigate the dynamical properties of neural networks, including stability, consensus, and dissipativity. Among these, synchronization is one of the most important. Since the finding of synchronization in chaotic dynamical systems [7], the synchronization of neural networks has been extensively investigated [8]–[12]. For instance, in [9], synchronization was studied for neural networks with state-dependent parameters. In [10], by using state-feedback control, fixed-time synchronization of neural networks was studied. In [11], event-triggered synchronization was investigated for coupled neural networks.

Under the assumption that all neurons of interest are fully mixed, most neural networks are represented by ordinary differential equations (ODEs). In these ODE models, the neuron states are dependent only on time, that is, only temporal evolution is considered, whereas spatial evolution is ignored. Reaction–diffusion processes are ubiquitous in a variety of technological applications, such as electric circuits, as well as in applications involving biological and chemical systems [13]–[17]. For example, in [14], by designing an image encryption algorithm, reaction–diffusion neural networks (RDNNs) were used for secure image communication. In [15], to better protect and control a population, RDNNs were used to model different population densities of species. The RDNNs introduced in [18] were applied to artificial locomotion [19]. Reaction–diffusion neural networks can effectively approximate the temporal and spatial movements of dynamical systems. They use the aforementioned ODE neural-network models and can exhibit more unpredictable and complex behavior. Recently, the synchronization of RDNNs has attracted considerable attention, resulting in a massive research output [20]–[24].

Various synchronization control strategies have been proposed for RDNNs, including feedback [25], adaptive [26], and pinning control [27]. These approaches are implemented by using continuous-time-feedback signals. However, in practice, digital-feedback signals are required for control schemes [28]. Therefore, sampled-data control (SDC) has attracted considerable attention [29]–[32]. It has more advantages than the existing control schemes, including simple structure, convenient installation, high reliability, and low cost. Recently, synchronization for RDNNs has been extensively studied by using SDC [33]–[36]. For instance, in [34], the exponential synchronization of fuzzy RDNNs was investigated using fuzzy SDC. Wang *et al.* [35] studied the synchronization problem for RDNNs through quantized SDC. In [36], the synchronization of reaction–diffusion FitzHugh–Nagumo systems was considered by using spatial SDC. Furthermore, owing to network-bandwidth limitations, it is difficult to utilize a sophisticated security system for network

Manuscript received 18 January 2022; accepted 6 April 2022. Date of publication 21 April 2022; date of current version 18 November 2022. This work was supported in part by the National Natural Science Foundation of China under Grant 62003229; in part by the Fundamental Research Funds for the Central Universities under Grant YJ202037; and in part by the Central Government Funds of Guiding Local Scientific and Technological Development for Sichuan Province of China under Grant 2021ZYD0012. The work of Ju H. Park was supported by the National Research Foundation of Korea (NRF) Grant funded by the Korea Government (Ministry of Science and ICT) under Grant 2019R1A5A8080290. This article was recommended by Associate Editor W. He. *(Corresponding authors: Hongxia Wang; Ju H. Park.)*

Ruimei Zhang, Hongxia Wang, and Peisong He are with the School of Cyber Science and Engineering, Sichuan University, Chengdu 610065, China (e-mail: ruimeizhang163@163.com; hxwang@scu.edu.cn; gokeyhps@scu.edu.cn).

Ju H. Park is with the Department of Electrical Engineering, Yeungnam University, Gyeongsan 38541, Republic of Korea (e-mail: jessie@ynu.ac.kr).

Hak-Keung Lam is with the Department of Engineering, King's College London, London WC2R 2LS, U.K. (e-mail: hak-keung.lam@kcl.ac.uk).

Color versions of one or more figures in this article are available at https://doi.org/10.1109/TSMC.2022.3166554.

Digital Object Identifier 10.1109/TSMC.2022.3166554

transmission. Cybersecurity risks are inevitable in network systems. Accordingly, cyberattacks have attracted considerable attention. For example, in [37], Denial-of-Service (DoS) attacks, in which the adversary attempts to prevent the availability of transmitted data at their terminal points by launching external jammers, were considered for cyber–physical systems. In [38]–[42], various types of deception attacks were studied, including replay attacks, false-data injection attacks, and data modification attacks. Unlike in DoS attacks, in deception attacks, the transmitted data can reach their destination, but the true values are replaced by false signals. Thus, deception attacks are stealthy and dangerous. They may degrade system performance, or even damage the system, by destroying the integrity of data resources. To save network bandwidth and improve the cybersecurity of communications, it is crucial to design an effective SDC scheme for RDNNs under deception attacks.

However, in existing studies on RDNNs [20]–[27], [33]–[36], it is assumed that there is no deception attack. Deception attacks have not been considered in the design of controllers, particularly when the time–space SDC mechanism is concurrently considered. Specifically, three difficulties are involved.

1) Deception attacks preclude a complete synchronization criterion for RDNNs. Then, the quasisynchronization problem should be considered. Quasisynchronization is a special type of synchronization pattern, in which all systems are almost synchronized with a given synchronization error [43].
2) Some existing approaches, such as the well-known Halanay's inequality [44], are useful for synchronization but not for quasisynchronization.
3) Time–space sampled-data (TSSD) signals and reaction–diffusion processes make it difficult to derive quasisynchronization criteria for RDNNs. To our knowledge, the quasisynchronization problem under deception attacks has not yet been investigated for RDNNs with time–space sampled data.

Motivated by the above, in this study, we focus on the quasisynchronization of RDNNs with time–space sampled data under deception attacks. The main contributions are as follows.

1) A time–space SDC mechanism is considered for RDNNs under deception attacks. This mechanism can save network bandwidth and improve the cybersecurity of communications.
2) Inspired by Halanay's inequality [44], a new inequality is proposed in Lemma 3. It is very helpful to solve the quasisynchronization problem for dynamical systems.
3) The quasisynchronization problem for RDNNs is studied, and new quasisynchronization criteria are provided.

Notations: For a matrix $\mathcal{X}$, $\mathrm{Sym}\{\mathcal{X}\}$ denotes the symmetric matrix obtained as $\mathcal{X}+\mathcal{X}^T$. Let $\mathscr{R}^{n\times n}$ denote the set of $n\times n$ real matrices, $\mathscr{R}^n$ be the n-dimensional Euclidean space, $\mathrm{col}\{\cdots\}$ be a column vector, $\lambda_{\min}(\cdot)$ be the minimum eigenvalue of a symmetric matrix, and $\mathrm{diag}\{\cdots\}$ be a block-diagonal matrix. For $\vartheta(s,x)\in\mathscr{R}^n$, the norm is denoted by $\|\vartheta(s,x)\| = (\int_{\underline{\kappa}}^{\bar{\kappa}} \vartheta^T(s,x)\vartheta(s,x)dx)^{(1/2)}$. 0_n, I_n, and $0_{n,m}$ stand for $n\times n$ zero matrices, $n\times n$ identity matrix, and $n\times m$ zero matrices, respectively.

II. Problem Formulation

Let us consider the following RDNN:

$$\begin{aligned}\frac{\partial\vartheta(t,x)}{\partial t} &= \mathcal{D}\frac{\partial^2\vartheta(t,x)}{\partial x^2} - \mathcal{C}\vartheta(t,x) + \mathcal{W}_1 f(\vartheta(t,x))\\ &\quad + \mathcal{W}_2 f(\vartheta(t-\tau(t),x)) + \mathcal{J}(t)\end{aligned}\tag{1}$$

where $t\in[\hat{t}_0,+\infty)$, $x\in\mho\triangleq\{x|\underline{\kappa}\le x\le\bar{\kappa}\}$ is the space variable, and $\underline{\kappa}$ and $\bar{\kappa}$ are constants. $\mathcal{D}=\mathrm{diag}\{d_1,d_2,\ldots,d_n\}$, $d_i>0$ $(i=1,2,\ldots,n)$ is the transmission diffusion coefficient. $\mathcal{C}=\mathrm{diag}\{c_1,c_2,\ldots,c_n\}$, with $c_i>0$. $\mathcal{W}_1=(w_{1,ij})_{n\times n}\in\mathscr{R}^{n\times n}$ and $\mathcal{W}_2=(w_{2,ij})_{n\times n}\in\mathscr{R}^{n\times n}$ are the connection strength matrices. $\vartheta(t,x)=\mathrm{col}\{\vartheta_1(t,x),\vartheta_2(t,x),\ldots,\vartheta_n(t,x)\}$ is the state vector, where $\vartheta_i(t,x)$ is the ith neuron in space x and at time t. $\tau(t)$ is the delay, with $\dot{\tau}(t)\le\mu<1$ and $0\le\tau(t)\le d^*$. $f(\vartheta(t,x))=\mathrm{col}\{f_1(\vartheta_1(t,x)),\ldots,f_n(\vartheta_n(t,x))\}$ is the neuron activation function. $\mathcal{J}(t)=\mathrm{col}\{\mathcal{J}_1(t),\mathcal{J}_2(t),\ldots,\mathcal{J}_n(t)\}$ is the input vector.

The Dirichlet boundary condition and the initial condition of system (1) are given as follows:

$$\vartheta(t,\underline{\kappa})=\vartheta(t,\bar{\kappa})=0,\quad t\in\big[\hat{t}_0,+\infty\big)\tag{2}$$

$$\vartheta\big(s+\hat{t}_0,x\big)=\phi_1(s,x)\in C\big(\big[-d^*,0\big]\times\mho,\mathscr{R}^n\big)\tag{3}$$

respectively, where $C([-d^*,0]\times\mho,\mathscr{R}^n)$ denotes the set of all continuous real-valued functions from $[-d^*,0]\times\mho$ to $\mathscr{R}^n$.

Regarding system (1) as the drive system, its response system is as follows:

$$\begin{aligned}\frac{\partial\upsilon(t,x)}{\partial t} &= \mathcal{D}\frac{\partial^2\upsilon(t,x)}{\partial x^2} - \mathcal{C}\upsilon(t,x) + \mathcal{W}_1 f(\upsilon(t,x))\\ &\quad + \mathcal{W}_2 f(\upsilon(t-\tau(t),x)) + \mathcal{U}(t,x) + \mathcal{J}(t)\end{aligned}\tag{4}$$

where $\upsilon(t,\underline{\kappa})=\upsilon(t,\bar{\kappa})=0$, $t\in[\check{t}_0,+\infty)$, $\upsilon(s+\check{t}_0,x)=\phi_2(s,x)\in C([-d^*,0]\times\mho,\mathscr{R}^n)$, and $\mathcal{U}(t,x)\in\mathscr{R}^n$ is the control signal.

We define the error signal $\delta(t,x)=\upsilon(t,x)-\vartheta(t,x)=\mathrm{col}\{\delta_1(t,x),\delta_2(t,x),\ldots,\delta_n(t,x)\}$. Then, from (1) and (4), the following error system is obtained:

$$\begin{aligned}\frac{\partial\delta(t,x)}{\partial t} &= \mathcal{D}\frac{\partial^2\delta(t,x)}{\partial x^2} - \mathcal{C}\delta(t,x) + \mathcal{W}_1 g(\delta(t,x))\\ &\quad + \mathcal{W}_2 g(\delta(t-\tau(t),x)) + \mathcal{U}(t,x)\end{aligned}\tag{5}$$

where $\delta(t,\underline{\kappa})=\delta(t,\bar{\kappa})=0$, $t\in[t_0,+\infty)$, $\delta(s+t_0,x)=\phi(s,x)\in C([-d^*,0]\times\mho,\mathscr{R}^n)$, and $g(\delta(t,x))=f(\upsilon(t,x))-f(\vartheta(t,x))$.

For $t\in[t_k,t_{k+1})$ and $x\in[x_p,x_{p+1})$, we consider the following TSSD controller:

$$\begin{cases}\mathcal{U}(t,x)=\mathcal{K}\delta\big(t_k,\bar{x}_p\big)\\ \bar{x}_p=\frac{x_p+x_{p+1}}{2}\end{cases}\tag{6}$$

where t_k is from a time-sampling sequence $t_0<t_1<\cdots<t_k<\cdots$, x_p is the space-sampling instant generated by dividing $\mho$ into m sampling intervals, with $\underline{\kappa}=x_0<x_1<\cdots<$

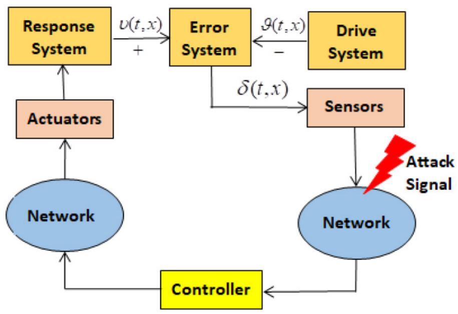

Fig. 1. Structure of drive–response RDNNs subjected to deception attacks.

$x_m = \bar{\kappa}$, and $\mathcal{K} \in \mathscr{R}^{n\times n}$ is the control gain to be designed. The time-sampling interval h_k satisfies the following:

$$0 < \underline{h} \le h_k \le \bar{h} \tag{7}$$

where $h_k = t_{k+1} - t_k$, and $\underline{h}$ and $\bar{h}$ are positive constants.

Inspired by [40]–[42] and [45], when the network channel between the sensor and the controller suffers bias-injection attacks, the TSSD controller under deception attacks can be modeled as follows:

$$\begin{aligned}\bar{\mathcal{U}}(t,x) &= \digamma\big(t_k,\bar{x}_p\big) + \mathcal{U}(t,x)\\ &= \mathcal{K}\tilde{\delta}\big(t_k,\bar{x}_p\big),\ \ t\in\big[t_k,t_{k+1}\big),\ \ x\in\big[x_p,x_{p+1}\big)\end{aligned} \tag{8}$$

where $\digamma(t_k,\bar{x}_p) \in \mathscr{R}^n$ is the injected attack signal sent by the attackers. As the attack resources of the adversary are limited, the constraint $\|\digamma(t_k,\bar{x}_p)\| \le \theta$ is required. Moreover, $\tilde{\delta}(t_k,\bar{x}_p) = \delta(t_k,\bar{x}_p) + G(t_k,\bar{x}_p)$ and $\digamma(t_k,\bar{x}_p) = \mathcal{K}G(t_k,\bar{x}_p)$. We note that the adversary's injection signal $\digamma(t_k,\bar{x}_p)$ will lead the control center to believe that the true network state is $\tilde{\delta}(t_k,\bar{x}_p)$. Fig. 1 shows the structure of drive–response systems subjected to deception attacks.

Replacing $\mathcal{U}(t,x)$ by $\bar{\mathcal{U}}(t,x)$, and combining (5) and (8), we obtain

$$\begin{aligned}\frac{\partial\delta(t,x)}{\partial t} &= \mathcal{D}\frac{\partial^2\delta(t,x)}{\partial x^2} - \mathcal{C}\delta(t,x) + \mathcal{W}_1 g(\delta(t,x))\\ &\quad + \mathcal{W}_2 g(\delta(t-\tau(t),x)) + \mathcal{K}\delta\big(t_k,\bar{x}_p\big)\\ &\quad + \digamma\big(t_k,\bar{x}_p\big),\ \ t\in\big[t_k,t_{k+1}\big),\ \ x\in\big[x_p,x_{p+1}\big)\\ \delta(t,\underline{\kappa}) &= \delta(t,\bar{\kappa}) = 0,\ \ t\in[t_0,+\infty)\\ \delta(s+t_0,x) &= \phi(s,x) \in C\big(\big[-d^*,0\big]\times\mho,\mathscr{R}^n\big).\end{aligned} \tag{9}$$

Remark 1: In practice, because of network-bandwidth limitations, it is necessary to reduce the network transmission signals. In SDC, signals are transmitted only at discrete-sampling points and, thus, the number of transmission signals can be effectively reduced. Moreover, it is well known that deception attacks are universal and dangerous, as they are intended to inject vicious data to degrade performance or even damage the system. However, the results of most existing studies on RDNNs [20]–[27], [33]–[36] were obtained under the assumption that there is no deception attack and, thus, they are invalid in the presence of such attacks. Hence, a TSSD controller under deception attacks is considered in (8). This controller can save network bandwidth and improve communications security in RDNNs.

Assumption 1 [25]: For any $s_1, s_2 \in \mathscr{R}$, there exist scalars l_i^- and l_i^+ such that $f_i(\cdot)$ in (1) satisfies

$$l_i^- \le \frac{f_i(s_1) - f_i(s_2)}{s_1 - s_2} \le l_i^+,\ \ s_1 \ne s_2,\ \ i = 1,2,\ldots,n.$$

Definition 1 [42]: Under deception attacks, the drive–response RDNNs (1) and (4) are quasisynchronous in the mean-square sense if there exists a bound $\varrho > 0$ such that the error signal $\delta(t,x)$ converges to the set

$$\mathfrak{S} = \Big\{\delta(t,x)\big|\|\delta(t,x)\|^2 \le \varrho\Big\}$$

as $t \to \infty$.

Lemma 1 [46]: For a continuously differentiable function $\varphi : [l_a, l_b] \to \mathscr{R}^n$ and a matrix $\mathscr{A} = \mathscr{A}^T \ge 0$, we have

$$-\int_{l_a}^{l_b}\dot{\varphi}^T(s)\mathscr{A}\dot{\varphi}(s)ds \le -\frac{1}{l_b - l_a}\big(\daleth_1^T\mathscr{A}\daleth_1 + 3\daleth_2^T\mathscr{A}\daleth_2\big)$$

where $\daleth_1 = \varphi(l_b) - \varphi(l_a)$ and $\daleth_2 = \varphi(l_b) + \varphi(l_a) - (2/l_b - l_a)\int_{l_a}^{l_b}\varphi(s)ds$.

Lemma 2 [47]: For $\mathscr{B} \ge 0 \in \mathscr{R}^{n\times n}$, and all functions $y \in C([\underline{\kappa},\bar{\kappa}],\mathscr{R}^n)$ with $y(\underline{\kappa}) = 0$ or $y(\bar{\kappa}) = 0$, the following inequality holds:

$$\int_{\underline{\kappa}}^{\bar{\kappa}} y^T(x)\mathscr{B}y(x)dx \le \frac{4\big(\bar{\kappa}-\underline{\kappa}\big)^2}{\pi^2}\int_{\underline{\kappa}}^{\bar{\kappa}}\dot{y}^T(x)\mathscr{B}\dot{y}(x)dx.$$

Furthermore, if $y(\underline{\kappa}) = y(\bar{\kappa}) = 0$, one has

$$\int_{\underline{\kappa}}^{\bar{\kappa}} y^T(x)\mathscr{B}y(x)dx \le \frac{\big(\bar{\kappa}-\underline{\kappa}\big)^2}{\pi^2}\int_{\underline{\kappa}}^{\bar{\kappa}}\dot{y}^T(x)\mathscr{B}\dot{y}(x)dx.$$

Lemma 3: Let $\nu > 0$, $\tau > 0$, and $0 < a < 2b$ be constants. If there exists an absolutely continuous function $\mathcal{V}(t)$:$[t_0 - \tau, +\infty) \to [0,+\infty)$ satisfying

$$\dot{\mathcal{V}}(t) + 2b\mathcal{V}(t) \le a\sup_{-\tau\le s\le 0}\mathcal{V}(t+s) + \nu,\ \ t \ge t_0$$

then

$$\mathcal{V}(t) \le e^{-2\alpha(t-t_0)}\sup_{-\tau\le s\le 0}\mathcal{V}(t_0+s) + \bar{\nu},\ \ t \ge t_0$$

where $\bar{\nu} = (\nu/[ae^{2\alpha\tau} + 2\alpha - a])$, and $\alpha > 0$ is the unique positive solution of $\alpha = b - (ae^{2\alpha\tau}/2)$.

Proof: Let $z(t) = e^{-2\alpha(t-t_0)}\sup_{-\tau\le s\le 0}\mathcal{V}(t_0+s) + \bar{\nu}$. One has

$$\mathcal{V}(t) < z(t),\ \ t\in[t_0-\tau,t_0]. \tag{10}$$

Thus, we should prove

$$\mathcal{V}(t) \le z(t),\ \ t \ge t_0. \tag{11}$$

If (11) does not hold, by the continuity of $\mathcal{V}(t)$, there exists $t^* > t_0$ such that

$$\begin{cases}\mathcal{V}(t) < z(t), & t\in\big[t_0-\tau,t^*\big)\\ \mathcal{V}(t^*) = z(t^*)\\ \dot{\mathcal{V}}(t^*) \ge \dot{z}(t^*).\end{cases} \tag{12}$$

It is noted that

$$\begin{aligned}\dot{z}(t) &= -2\alpha z(t) + 2\alpha\bar{\nu}\\ &= -2bz(t) + ae^{2\alpha\tau}z(t) + 2\alpha\bar{\nu}\\ &= -2bz(t) + az(t-\tau) + ae^{2\alpha\tau}\bar{\nu} - a\bar{\nu} + 2\alpha\bar{\nu}.\end{aligned} \tag{13}$$

Then, from (13), one has

$$\begin{aligned}\dot{\mathcal{V}}(t^*) &\le -2b\mathcal{V}(t^*) + a \sup_{-\tau\le s\le 0} \mathcal{V}(t^*+s) + \nu \\ &= -2bz(t^*) + a \sup_{t^*-\tau\le s\le t^*} \mathcal{V}(s) + \nu \\ &< -2bz(t^*) + a \sup_{t^*-\tau\le s\le t^*} z(s) + \nu \\ &= -2bz(t^*) + a \sup_{t^*-\tau\le s\le t^*} \Big\{ e^{-2\alpha(s-t_0)} \\ &\qquad \times \sup_{-\tau\le s_1\le 0} \mathcal{V}(t_0+s_1) + \bar{\nu} \Big\} + \nu \\ &= -2bz(t^*) + ae^{-2\alpha(t^*-\tau-t_0)} \sup_{-\tau\le s\le 0} \mathcal{V}(t_0+s) \\ &\quad + a\bar{\nu} + \nu \\ &= -2bz(t^*) + az(t^*-\tau) + \nu \\ &= \dot{z}(t^*) - \left(ae^{2\alpha\tau} - a + 2\alpha\right)\bar{\nu} + \nu \\ &= \dot{z}(t^*) \end{aligned} \tag{14}$$

which contradicts (12). Thus, (11) holds ■

Remark 2: Note that Lemma 3 is newly proposed and can be effectively applied to the quasisynchronization problem for dynamic systems. When $\nu = 0$, the inequality is reduced to Halanay's inequality [44] and, thus, Halanay's inequality is a special case of Lemma 3. However, Halanay's inequality is not applicable to the quasisynchronization problem. It should be noted that a new inequality was proposed for quasisynchronization of delayed memristive neural networks in [48, Lemma 4]. By comparing Lemma 4 of [48] and Lemma 3 in this study, the following can be concluded.

1) In [48, Lemma 4], $\mathcal{V}(t)$ is required to satisfy $\dot{\mathcal{V}}(t) \le -2b\mathcal{V}(t)+a\mathcal{V}(t-\tau(t))+\nu$, where $\tau(t) \le \tau$. However, in Lemma 3 of this study, $\mathcal{V}(t)$ is required to satisfy $\dot{\mathcal{V}}(t) \le -2b\mathcal{V}(t)+a\sup_{-\tau\le s\le 0}\mathcal{V}(t+s)+\nu$. It is clear that $\dot{\mathcal{V}}(t) \le -2b\mathcal{V}(t)+a\mathcal{V}(t-\tau(t))+\nu$ implies $\dot{\mathcal{V}}(t) \le -2b\mathcal{V}(t)+a\sup_{-\tau\le s\le 0}\mathcal{V}(t+s)+\nu$, but not conversely. Thus, the required condition in Lemma 4 of [48] is stronger than that in Lemma 3 of this study.
2) In [48, Lemma 4], $\bar{\nu} = (\nu/2\alpha)$, whereas in Lemma 3 of this study, $\bar{\nu} = (\nu/2b-a)$. The condition $\alpha = b - (ae^{2\alpha\tau}/2)$ implies $(\nu/2\alpha) > (\nu/2b-a)$. Thus, Lemma 3 in this study provides a tighter quasisynchronization error bound than that by Lemma 4 of [48].

Hence, the inequality in Lemma 3 of this study is less conservative.

III. Main Results

We study the quasisynchronization of RDNNs under deception attacks by using time–space SDC. We first derive sufficient conditions for the drive–response systems (1) and (4) to be quasisynchronized. Subsequently, we design the TSSD controller (8). In addition, we study the exponential synchronization problem for RDNNs in the absence of deception attacks.

A. Quasisynchronization for RDNNs Under Deception Attacks

Herein, a new quasisynchronization criterion is derived for RDNNs by selecting an appropriate Lyapunov–Krasovskii functional (LKF). Let $\sigma(t) = t - t_k$, $L^+ = \mathrm{diag}\{l_1^+, l_2^+, \ldots, l_n^+\}$, $L^- = \mathrm{diag}\{l_1^-, l_2^-, \ldots, l_n^-\}$, $\mathcal{I}_i = [0_{n,(i-1)n} \;\; I_n \;\; 0_{n,(7-i)n}], (i = 1, \ldots, 7)$, and $\eta(t,x) = \mathrm{col}\{\delta(t,x),\ \delta(t_k,x),\ g(\delta(t,x)),\ (\partial\delta(t,x)/\partial t),\ (1/t-t_k)\int_{t_k}^{t}\delta(s,x)ds,\ \delta(t-\tau(t),x),\ g(\delta(t-\tau(t),x))\}$.

Theorem 1: Let scalars $\underline{h} > 0$, $\bar{h} > 0$, $\rho > 0$, $\theta > 0$, $0 < a < 2\alpha \le 2\epsilon$, and $m^* > 0$ be given. If there exist diagonal matrices $\Gamma_i > 0 \in \mathscr{R}^{n\times n}(i = 1, 2)$, matrices $\mathcal{H} > 0 \in \mathscr{R}^{n\times n}$, $\mathcal{H} \ge m^* I_n$, $\mathcal{M} > 0 \in \mathscr{R}^{n\times n}$, $\mathcal{P} > 0 \in \mathscr{R}^{n\times n}$, $\mathcal{Q} > 0 \in \mathscr{R}^{n\times n}$, $\mathcal{R} > 0 \in \mathscr{R}^{n\times n}$, $\mathcal{S} > 0 \in \mathscr{R}^{n\times n}$, $\mathcal{T}_i > 0 \in \mathscr{R}^{n\times n}(i = 1, 2)$, and any matrices $\mathcal{N} \in \mathscr{R}^{n\times n}$, $\mathcal{Y}_1 \in \mathscr{R}^{n\times 2n}$, $\mathcal{Y}_2 \in \mathscr{R}^{n\times 3n}$, for any $h_k \in \{\underline{h}, \bar{h}\}$ satisfying $\mathcal{N}\mathcal{D} > 0$ and

$$\begin{bmatrix} -\rho I_n & \mathcal{N}^T \\ * & -\mathcal{T}_2 \end{bmatrix} \le 0 \tag{15}$$

$$\begin{bmatrix} -a\mathcal{N}\mathcal{D} & (\mathcal{N}\mathcal{K})^T \\ * & -\frac{\pi^2}{\tilde{h}_x^2}\mathcal{T}_1 \end{bmatrix} \le 0 \tag{16}$$

$$\Psi^*(0; h_k, 0) < 0 \tag{17}$$

$$\begin{bmatrix} \Psi^*(0; h_k, h_k) & [\mathcal{I}_1^T, \mathcal{I}_2^T]\mathcal{Y}_1^T & [\mathcal{I}_1^T, \mathcal{I}_2^T, \mathcal{I}_5^T]\mathcal{Y}_2^T \\ * & -\frac{e^{2\alpha\bar{h}}}{h_k}\mathcal{P} & 0 \\ * & * & -\frac{e^{2\alpha\bar{h}}}{3h_k}\mathcal{P} \end{bmatrix} < 0. \tag{18}$$

Then, the drive–response RDNNs (1) and (4) are quasisynchronous in the mean-square sense, and the error signal $\delta(t,x)$ converges to the set

$$\mathfrak{S} = \left\{\delta(t,x) \,|\, \|\delta(t,x)\|^2 \le \varrho\right\} \tag{19}$$

where $\varrho = (\bar{m}/m^*)(1 + [1/1 - e^{-\xi\underline{h}}])$, $\xi = \alpha - (ae^{2\xi\tau}/2)$, $\bar{m} = (\rho\theta^2/ae^{2\xi\tau} + 2\xi - a)$, $\Psi^*(\iota; h_k, \sigma(t)) = \Psi(\iota; h_k, \sigma(t)) - a\mathcal{I}_2^T\mathcal{H}\mathcal{I}_2$, and $\tilde{h}_x = \max_{0\le p\le m-1}\{x_{p+1} - x_p\}$, with $\Psi(\iota; h_k, \sigma(t)) = \sum_{i=1}^{3} \Psi_k(\iota; h_k, \sigma(t))$ and

$$\begin{aligned} &\Psi_1(\iota; h_k, \sigma(t)) \\ &= 2\alpha\mathcal{I}_1^T\mathcal{H}\mathcal{I}_1 + \mathrm{Sym}\{\mathcal{I}_1^T\mathcal{H}\mathcal{I}_4\} + \mathcal{I}_1^T\mathcal{M}\mathcal{I}_1 + \mathcal{I}_3^T\mathcal{Q}\mathcal{I}_3 \\ &\quad - (1-\mu)e^{-2\alpha\tau}\mathcal{I}_6^T\mathcal{M}\mathcal{I}_6 - (1-\mu)e^{-2\alpha\tau}\mathcal{I}_7^T\mathcal{Q}\mathcal{I}_7 \\ &\quad + \frac{2(\alpha-\epsilon)\pi^2}{(\bar{\kappa}-\underline{\kappa})^2}\mathcal{I}_1^T\mathcal{N}\mathcal{D}\mathcal{I}_1 + (h_k - \sigma(t))\mathcal{I}_4^T\mathcal{P}\mathcal{I}_4 \\ &\quad + \iota e^{-2\alpha\bar{h}}\sigma(t)[\mathcal{I}_1^T, \mathcal{I}_2^T]\mathcal{Y}_1^T\mathcal{P}^{-1}\mathcal{Y}_1[\mathcal{I}_1^T, \mathcal{I}_2^T]^T \\ &\quad + 3\iota e^{-2\alpha\bar{h}}\sigma(t)[\mathcal{I}_1^T, \mathcal{I}_2^T, \mathcal{I}_5^T]\mathcal{Y}_2^T\mathcal{P}^{-1}\mathcal{Y}_2[\mathcal{I}_1^T, \mathcal{I}_2^T, \mathcal{I}_5^T]^T \\ &\quad - e^{-2\alpha\bar{h}}\mathrm{Sym}\left\{(\mathcal{I}_1 - \mathcal{I}_2)^T\mathcal{Y}_1[\mathcal{I}_1^T, \mathcal{I}_2^T]^T\right\} \\ &\quad - 3e^{-2\alpha\bar{h}}\mathrm{Sym}\left\{(\mathcal{I}_1 + \mathcal{I}_2 - 2\mathcal{I}_5)^T\mathcal{Y}_2[\mathcal{I}_1^T, \mathcal{I}_2^T, \mathcal{I}_5^T]^T\right\} \\ &\quad + 2\alpha(h_k - \sigma(t))(\mathcal{I}_1 - \mathcal{I}_2)^T\mathcal{R}(\mathcal{I}_1 - \mathcal{I}_2) \\ &\quad - (\mathcal{I}_1 - \mathcal{I}_2)^T\mathcal{R}(\mathcal{I}_1 - \mathcal{I}_2) \\ &\quad + (h_k - \sigma(t))\mathrm{Sym}\{(\mathcal{I}_1 - \mathcal{I}_2)^T\mathcal{R}\mathcal{I}_4\} \\ &\quad + \frac{\alpha\bar{h}^2}{2}\mathcal{I}_5^T\mathcal{S}\mathcal{I}_5 + (h_k - 2\sigma(t))\mathcal{I}_5^T\mathcal{S}\mathcal{I}_5 \end{aligned}$$

$$+ (h_k - \sigma(t))\mathrm{Sym}\{\mathcal{I}_5^T \mathcal{S}(-\mathcal{I}_5 + \mathcal{I}_1)\}$$

$$\Psi_2(\iota; h_k, \sigma(t)) = \mathrm{Sym}\Big\{\big(\mathcal{I}_3 - L^- \mathcal{I}_1\big)^T \Gamma_1 \big(L^+ \mathcal{I}_1 - \mathcal{I}_3\big)\Big\} + \mathrm{Sym}\Big\{\big(\mathcal{I}_7 - L^- \mathcal{I}_6\big)^T \Gamma_2 \big(L^+ \mathcal{I}_6 - \mathcal{I}_7\big)\Big\}$$

$$\Psi_3(\iota; h_k, \sigma(t)) = \mathrm{Sym}\{(\mathcal{I}_4^T + \epsilon \mathcal{I}_1^T)\mathcal{N}(-\mathcal{I}_4 - \mathcal{C}\mathcal{I}_1 + \mathcal{W}_1\mathcal{I}_3 + \mathcal{W}_2\mathcal{I}_7)\} + \mathrm{Sym}\{(\mathcal{I}_4^T + \epsilon \mathcal{I}_1^T)\mathcal{N}\mathcal{K}\mathcal{I}_2\} + (\mathcal{I}_4 + \epsilon\mathcal{I}_1)^T \mathcal{T}_1 (\mathcal{I}_4 + \epsilon\mathcal{I}_1) + (\mathcal{I}_4 + \epsilon\mathcal{I}_1)^T \mathcal{T}_2 (\mathcal{I}_4 + \epsilon\mathcal{I}_1).$$

Proof: See the Appendix. ■

Remark 3: As is well known, by Lyapunov stability theory, constructing a suitable LKF for deriving synchronization criteria is crucial. In this study, (29) is constructed as the LKF, where $\mathcal{V}_1(t)$ is generally needed, $\mathcal{V}_2(t)$ is constructed to capture the information of the activation function $g(\delta(\cdot, x))$, and $\mathcal{V}_3(t)$ is used to counteract the term $2\sum_{p=0}^{m-1}\int_{x_p}^{x_{p+1}}(\partial\delta^T(t,x)/\partial t)\mathcal{N}\mathcal{D}(\partial\delta^2(t,x)/\partial x^2)dx$ in (44). For SDC systems, sampling information is useful in reducing the conservatism of synchronization criteria. In this regard, the sawtooth structure terms $\mathcal{V}_i(t)$ $(i = 4, 5, 6)$ are introduced to capture sampling information.

Remark 4: In the defect of deception attacks, obtaining a complete synchronization criterion for RDNNs is impossible. Furthermore, to our knowledge, there is no result on the quasisynchronization of RDNNs with time–space sampled data under deception attacks. This issue is addressed in the present study. By constructing the LKF in (29) and using the new inequality in Lemma 3, a novel quasisynchronization criterion is established for RDNNs in Theorem 1.

B. Time–Space Sampled-Data Controller Design

Note that Theorem 1 is not linear matrix inequalities (LMIs), as the terms $(\mathcal{N}\mathcal{K})^T$ and $\mathrm{Sym}\{(\mathcal{I}_4^T + \epsilon\mathcal{I}_1^T)\mathcal{N}\mathcal{K}\mathcal{I}_2\}$ are not linear. The TSSD controller cannot be directly obtained by the conditions in Theorem 1. Rather, the TSSD controller is designed in the following theorem by converting the nonlinear inequalities of Theorem 1 into linear inequalities.

Theorem 2: Let scalars $\underline{h} > 0$, $\bar{h} > 0$, $\rho > 0$, $\theta > 0$, $0 < a < 2\alpha \leq 2\epsilon$, and $m^* > 0$ be given. If there exist diagonal matrices $\Gamma_i > 0 \in \mathscr{R}^{n\times n} (i = 1, 2)$, matrices $\mathcal{H} > 0 \in \mathscr{R}^{n\times n}$, $\mathcal{H} \geq m^* I_n$, $\mathcal{M} > 0 \in \mathscr{R}^{n\times n}$, $\mathcal{P} > 0 \in \mathscr{R}^{n\times n}$, $\mathcal{Q} > 0 \in \mathscr{R}^{n\times n}$, $\mathcal{R} > 0 \in \mathscr{R}^{n\times n}$, $\mathcal{S} > 0 \in \mathscr{R}^{n\times n}$, $\mathcal{T}_i > 0 \in \mathscr{R}^{n\times n} (i = 1, 2)$, and any matrices $\mathcal{N} \in \mathscr{R}^{n\times n}$, $\mathcal{K}^* \in \mathscr{R}^{n\times n}$, $\mathcal{Y}_1 \in \mathscr{R}^{n\times 2n}$, $\mathcal{Y}_2 \in \mathscr{R}^{n\times 3n}$, for any $h_k \in \{\underline{h}, \bar{h}\}$ satisfying $\mathcal{N}\mathcal{D} > 0$ and

$$\begin{bmatrix} -\rho I_n & \mathcal{N}^T \\ * & -\mathcal{T}_2 \end{bmatrix} \leq 0 \tag{20}$$

$$\begin{bmatrix} -a\mathcal{N}\mathcal{D} & \mathcal{K}^{*T} \\ * & -\frac{\pi^2}{\bar{h}_x^2}\mathcal{T}_1 \end{bmatrix} \leq 0 \tag{21}$$

$$\Psi^{**}(0; h_k, 0) < 0 \tag{22}$$

$$\begin{bmatrix} \Psi^{**}(0; h_k, h_k) & [\mathcal{I}_1^T, \mathcal{I}_2^T]\mathcal{Y}_1^T & [\mathcal{I}_1^T, \mathcal{I}_2^T, \mathcal{I}_5^T]\mathcal{Y}_2^T \\ * & -\frac{e^{2\alpha\bar{h}}}{h_k}\mathcal{P} & 0 \\ * & * & -\frac{e^{2\alpha\bar{h}}}{3h_k}\mathcal{P} \end{bmatrix} < 0 \tag{23}$$

then the drive–response RDNNs (1) and (4) are quasisynchronous in the mean-square sense, and the error signal $\delta(t, x)$ converges to the set $\mathfrak{S}$ in (19), where $\Psi^{**}(\iota; h_k, \sigma(t)) = \tilde{\Psi}(\iota; h_k, \sigma(t)) - a\mathcal{I}_2^T\mathcal{H}\mathcal{I}_2$ and $\tilde{\Psi}(\iota; h_k, \sigma(t)) = \sum_{i=1}^{2}\Psi_k(\iota; h_k, \sigma(t)) + \tilde{\Psi}_3(\iota; h_k, \sigma(t))$, with

$$\tilde{\Psi}_3(\iota; h_k, \sigma(t)) = \mathrm{Sym}\{(\mathcal{I}_4^T + \epsilon\mathcal{I}_1^T)\mathcal{N}(-\mathcal{I}_4 - \mathcal{C}\mathcal{I}_1 + \mathcal{W}_1\mathcal{I}_3 + \mathcal{W}_2\mathcal{I}_7)\} + \mathrm{Sym}\{(\mathcal{I}_4^T + \epsilon\mathcal{I}_1^T)\mathcal{K}^*\mathcal{I}_2\} + (\mathcal{I}_4 + \epsilon\mathcal{I}_1)^T\mathcal{T}_1(\mathcal{I}_4 + \epsilon\mathcal{I}_1) + (\mathcal{I}_4 + \epsilon\mathcal{I}_1)^T\mathcal{T}_2(\mathcal{I}_4 + \epsilon\mathcal{I}_1)$$

and other notations as in Theorem 1. Furthermore, the TSSD controller gain for (8) is given as follows:

$$\mathcal{K} = \mathcal{N}^{-1}\mathcal{K}^*. \tag{24}$$

Proof: Let $\mathcal{N}\mathcal{K} = \mathcal{K}^*$. Then, Theorem 1 implies that (20)–(23) hold. The proof is completed. ■

C. Exponential Synchronization for RDNNs

In defect of deception attacks, the error system (9) is reduced to

$$\begin{aligned} \frac{\partial\delta(t,x)}{\partial t} &= \mathcal{D}\frac{\partial^2\delta(t,x)}{\partial x^2} - \mathcal{C}\delta(t,x) + \mathcal{W}_1 g(\delta(t,x)) \\ &\quad + \mathcal{W}_2 g(\delta(t-\tau(t),x)) + \mathcal{K}\delta(t_k, \bar{x}_p) \\ &\quad t \in [t_k, t_{k+1}),\ x \in [x_p, x_{p+1}) \\ \delta(t, \underline{\kappa}) &= \delta(t, \bar{\kappa}) = 0,\ t \in [t_0, +\infty) \\ \delta(s + t_0, x) &= \phi(s, x) \in C([-d^*, 0] \times \mho, \mathscr{R}^n). \end{aligned} \tag{25}$$

Let $m^* = \lambda_{\min}(\mathcal{H})$ and $\theta = 0$. As in the proof of Theorem 1, we have the exponential synchronization condition for RDNNs (1) and (4) as follows.

Corollary 1: Let scalars $\underline{h} > 0$, $\bar{h} > 0$, and $0 < a < 2\alpha \leq 2\epsilon$ be given. The drive–response RDNNs (1) and (4) are exponentially synchronized if there exist diagonal matrices $\Gamma_i > 0 \in \mathscr{R}^{n\times n} (i = 1, 2)$, matrices $\mathcal{H} > 0 \in \mathscr{R}^{n\times n}$, $\mathcal{M} > 0 \in \mathscr{R}^{n\times n}$, $\mathcal{P} > 0 \in \mathscr{R}^{n\times n}$, $\mathcal{Q} > 0 \in \mathscr{R}^{n\times n}$, $\mathcal{R} > 0 \in \mathscr{R}^{n\times n}$, $\mathcal{S} > 0 \in \mathscr{R}^{n\times n}$, $\mathcal{T}_1 > 0 \in \mathscr{R}^{n\times n}$, and any matrices $\mathcal{N} \in \mathscr{R}^{n\times n}$, $\mathcal{K}^* \in \mathscr{R}^{n\times n}$, $\mathcal{Y}_1 \in \mathscr{R}^{n\times 2n}$, $\mathcal{Y}_2 \in \mathscr{R}^{n\times 3n}$, for any $h_k \in \{\underline{h}, \bar{h}\}$ satisfying $\mathcal{N}\mathcal{D} > 0$, (21), and

$$\hat{\Psi}^{**}(0; h_k, 0) < 0 \tag{26}$$

$$\begin{bmatrix} \hat{\Psi}^{**}(0; h_k, h_k) & [\mathcal{I}_1^T, \mathcal{I}_2^T]\mathcal{Y}_1^T & [\mathcal{I}_1^T, \mathcal{I}_2^T, \mathcal{I}_5^T]\mathcal{Y}_2^T \\ * & -\frac{e^{2\alpha\bar{h}}}{h_k}\mathcal{P} & 0 \\ * & * & -\frac{e^{2\alpha\bar{h}}}{3h_k}\mathcal{P} \end{bmatrix} < 0 \tag{27}$$

where $\hat{\Psi}^{**}(\iota; h_k, \sigma(t)) = \hat{\Psi}(\iota; h_k, \sigma(t)) - a\mathcal{I}_2^T\mathcal{H}\mathcal{I}_2$ and $\hat{\Psi}(\iota; h_k, \sigma(t)) = \sum_{i=1}^{2}\Psi_k(\iota; h_k, \sigma(t)) + \hat{\Psi}_3(\iota; h_k, \sigma(t))$, with

$$\hat{\Psi}_3(\iota; h_k, \sigma(t)) = \mathrm{Sym}\{(\mathcal{I}_4^T + \epsilon\mathcal{I}_1^T)\mathcal{N}(-\mathcal{I}_4 - \mathcal{C}\mathcal{I}_1 + \mathcal{W}_1\mathcal{I}_3 + \mathcal{W}_2\mathcal{I}_7)\} + \mathrm{Sym}\{(\mathcal{I}_4^T + \epsilon\mathcal{I}_1^T)\mathcal{K}^*\mathcal{I}_2\} + (\mathcal{I}_4 + \epsilon\mathcal{I}_1)^T\mathcal{T}_1(\mathcal{I}_4 + \epsilon\mathcal{I}_1)$$

and other notations as in Theorem 1. Furthermore, the TSSD controller gain for (6) is given as follows:

$$\mathcal{K} = \mathcal{N}^{-1}\mathcal{K}^*. \tag{28}$$

Remark 5: It should be noted that the quasisynchronization criterion in Theorem 2 and the synchronization criterion in Corollary 1 are LMIs. In LMI conditions, the number of decision variables (NDVs) and the dimensions of the LMIs are important factors affecting the complexity of computing [49]. In general, the NDV is a measure of the complexity of computing. The NDVs in Theorem 2 and Corollary 1 are $11n^2+6n$ and $10.5n^2+5.5n$, respectively. When the size of the LMIs increases, the computational complexity may be a problem because of limited computational resources. Thus, for high-dimensional LMI conditions, calculation complexity should be maintained at a reasonable level.

Remark 6: The proposed sufficient conditions in Theorem 2 and Corollary 1 are in the form of LMIs and can be verified through the following steps.

Step 1: For given $0 < a < 2\alpha \le 2\epsilon$, $m^* > 0$, $\rho > 0$, and $\theta > 0$, specify the ranges $\bar{h}$ in increments of $\Delta\bar{h} > 0$. Set $\bar{h} = \Delta\bar{h}$.

Step 2: Use MATLAB LMI Toolbox to solve the LMIs in Theorem 2 with specified $\bar{h}$.

Step 3: If there is a feasible solution, let $\bar{h} = \bar{h} + \Delta\bar{h}$ and carry out step 2; if not, carry out step 4.

Step 4: If $h = \Delta h$, output "No feasible solutions." Then, reselect $0 < a < 2\alpha \le 2\epsilon$, $m^* > 0$, $\rho > 0$, and $\theta > 0$, and carry out step 1; if not, carry out step 5.

Step 5: Output $\bar{h} = \bar{h} - \Delta\bar{h}$, which is the maximum time-sampling interval (MTSI). With this $\bar{h}$ and using MATLAB LMI Toolbox to solve the LMIs in Theorem 2, one gets the feasible matrices. Then, from (24), we obtain the time–space SDC gains $\mathcal{K}$.

The LMI conditions of Corollary 1 can be verified similarly.

IV. Simulation Examples

Here, two examples are presented to demonstrate the usefulness of the theoretical results.

Example 1: Let us consider the RDNN (1) with parameters as follows:

$$\mathcal{D} = \begin{bmatrix} 0.6 & 0 \\ 0 & 0.6 \end{bmatrix}, \quad \mathcal{C} = I_2$$
$$\mathcal{W}_1 = \begin{bmatrix} 2 & -0.1 \\ -5 & 3 \end{bmatrix}, \quad \mathcal{W}_2 = \begin{bmatrix} -1.5 & -0.1 \\ -0.2 & -2.5 \end{bmatrix}$$
$$f_i(\vartheta_i(t,x)) = \tanh(\vartheta_i(t,x)) \ (i = 1, 2)$$
$$\mho = \{x \mid -1 \le x \le 5\}, \ \tau(t) = 1, \ \mathcal{J}(t) = 0.$$

It is clear that $l_1^+ = l_2^+ = 1$ and $l_1^- = l_2^- = 0$. In this example, we take $\alpha = 0.6$, $a = 0.9956$, $\epsilon = 7$, and the initial condition of system (1) is $\phi_{11}(s,x) = 0.5\cos(\pi(x-2)/6)$ and $\phi_{12}(s,x) = -0.9\cos(\pi(x-2)/6)$. The initial condition of the response RDNN (4) is $\phi_{21}(s,x) = 0.475\cos(\pi(x-2)/6)$ and $\phi_{22}(s,x) = -0.945\cos(\pi(x-2)/6)$; moreover, (4) has the same structure as system (1).

The following two cases are now discussed.

Case 1: Quasisynchronization for RDNNs (1) and (4) under deception attacks.

Case 2: Exponential synchronization for RDNNs (1) and (4) without deception attacks.

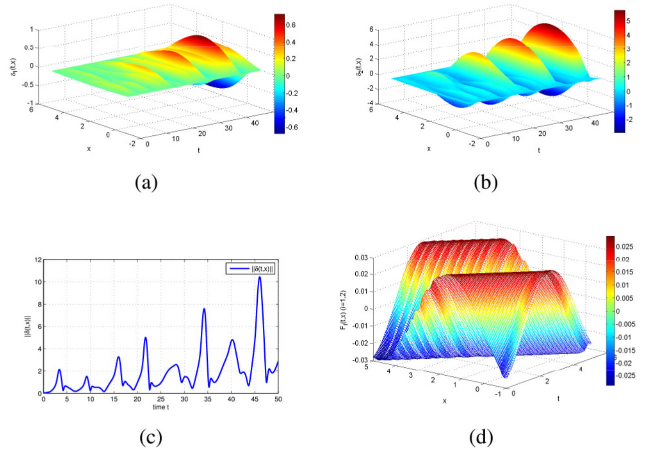

Fig. 2. Trajectories of uncontrolled states and attack signal: (a) $\delta_1(t,x)$, (b) $\delta_2(t,x)$, (c) $\|\delta(t,x)\|$, and (d) attack signal $\digamma_i(t_k, \bar{x}_p)$.

In case 1, we set the attack signal $\digamma_i(t_k, \bar{x}_p) = (\theta/2\sqrt{3})\sin(t_k + \bar{x}_p)$ $(i = 1, 2)$ and select $\theta = 0.1$, $\rho = 1$, $m^* = 3$, $\tilde{h}_x = 0.1$, and $\bar{h} = \underline{h} = 0.0438$. When $\mathcal{U}(t,x) = 0$, the trajectories of $\delta_1(t,x)$ and $\delta_2(t,x)$, and the error signal $\|\delta(t,x)\|$ are shown in Fig. 2(a)–(c). The dynamical behavior of the attack signal $\digamma_i(t_k, \bar{x}_p)$ is shown in Fig. 2(d). It can be seen from Fig. 2(a)–(c) that, under deception attacks, the quasisynchronization of systems (1) and (4) cannot be accomplished without control input.

Now, we check the effectiveness of Theorem 2. Following the steps in Remark 6, one obtains the following feasible solutions (to save space, some of the matrices are not listed):

$$\mathcal{H} = \begin{bmatrix} 3.4370 & 0.1399 \\ 0.1399 & 3.0455 \end{bmatrix}, \ \mathcal{M} = \begin{bmatrix} 4.5530 & 1.2800 \\ 1.2800 & 0.7502 \end{bmatrix},$$
$$\mathcal{N} = \begin{bmatrix} 0.4164 & -0.0470 \\ -0.0060 & 0.3104 \end{bmatrix}, \ \mathcal{K}^* = \begin{bmatrix} -4.7048 & 0.2592 \\ 0.7182 & -4.4038 \end{bmatrix}.$$

Then, from (24), the desired time–space SDC gain is obtained as follows:

$$\mathcal{K} = \begin{bmatrix} -11.0625 & -0.9801 \\ 2.1014 & -14.2061 \end{bmatrix}.$$

With the above parameters, Fig. 3 shows the controlled time–space behavior of states $\delta_i(t,x)$ $(i = 1, 2)$ and the TSSD controller $\mathcal{U}(t,x)$. The evolution of the controlled error signal $\|\delta(t,x)\|$ is plotted in Fig. 4, where it can be seen that the drive-response RDNNs (1) and (4) are quasisynchronous in the mean-square sense, with the error signal $\delta(t,x)$ converging to the set $\mathfrak{S} = \{\delta(t,x) \mid \|\delta(t,x)\|^2 \le 3.7483\}$. Thus, the effectiveness of Theorem 2 is verified.

Then, we demonstrate the effect of deception attacks on the quasisynchronization of RDNNs (1) and (4). For various θ, the corresponding quasisynchronization bounds ϱ are given in Table I, where it can be seen that ϱ increases with θ. This implies that deception attacks affect the dynamics of the considered RDNNs. Moreover, for different values of θ, the evolution of $\|\delta(t,x)\|$ is shown in Fig. 5.

In case 2, we take $\theta = 0$. For various space-sampling intervals $\tilde{h}_x$, the corresponding MTSI $\bar{h}$ is listed in Table II. From Table II, one finds that as $\tilde{h}_x$ increases, $\bar{h}$ decreases.

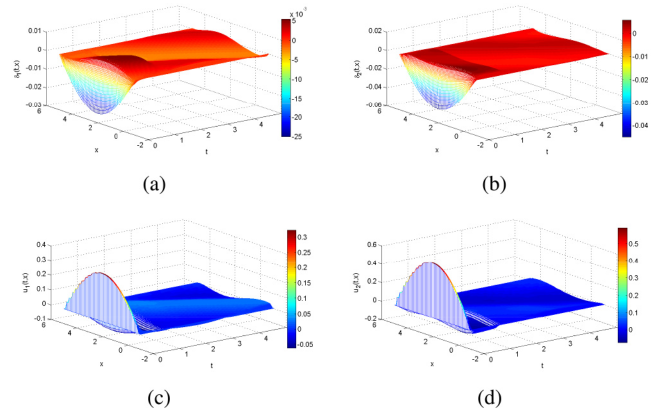

Fig. 3. Behavior of controlled states for error system (5) and the corresponding TSSD controller: (a) $\delta_1(t,x)$, (b) $\delta_2(t,x)$, (c) $\mathcal{U}_1(t,x)$, and (d) $\mathcal{U}_2(t,x)$.

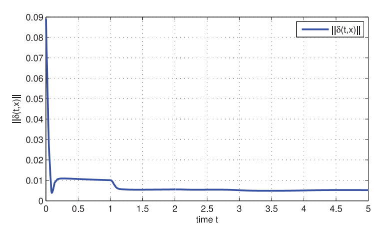

Fig. 4. Evolution of error signal $\|\delta(t,x)\|$ with $\mathcal{U}(t,x)$.

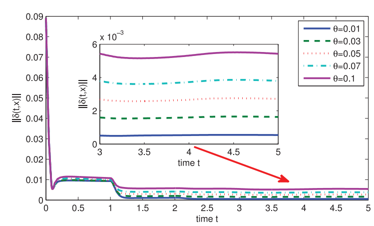

Fig. 5. Evolution of error signal $\|\delta(t,x)\|$ for various θ of the deception attacks.

TABLE I
QUASISYNCHRONIZATION BOUND ϱ FOR VARIOUS θ OF THE DECEPTION ATTACKS IN CASE 1

θ	0.01	0.03	0.05	0.07	0.1
ϱ	0.0375	0.3373	0.9371	1.8367	3.7483

TABLE II
MTSI $\bar{h}$ FOR VARIOUS SPACE-SAMPLING INTERVALS $\tilde{h}_x$ IN CASE 2

$\tilde{h}_x$	0.1	0.12	0.15	0.17	0.2
$\bar{h}$	0.0690	0.0624	0.0499	0.0397	0.0203

When $\tilde{h}_x = 0.2$ and $\bar{h} = 0.0203$, by Corollary 1, one obtains the following time–space SDC gain:

$$\mathcal{K} = \begin{bmatrix} -9.4739 & -1.3766 \\ 1.8696 & -11.9591 \end{bmatrix}.$$

Without control input, the state trajectory of the error signal $\|\delta(t,x)\|$ of system (25) is shown in Fig. 6 (a). Then, with the above parameters and control gain, the evolution of $\|\delta(t,x)\|$ is shown in Fig. 6 (b), where it is seen that the error signal $\|\delta(t,x)\|$ converges to zero only in the presence of the TSSD controller $\mathcal{U}(t,x)$. This indicates the effectiveness of Corollary 1.

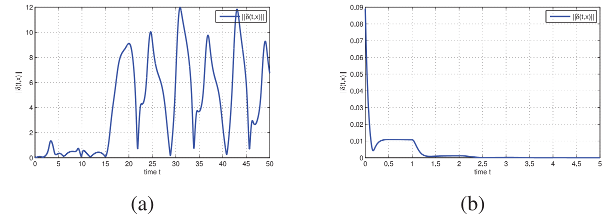

Fig. 6. Evolution of error signal $\|\delta(t,x)\|$ of system (25): (a) $\|\delta(t,x)\|$ without control input and (b) $\|\delta(t,x)\|$ with TSSD controller $\mathcal{U}(t,x)$.

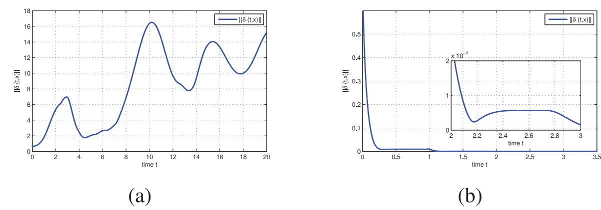

Fig. 7. Evolution of error signal $\|\delta(t,x)\|$: (a) $\|\delta(t,x)\|$ without control input and (b) $\|\delta(t,x)\|$ with controller $\mathcal{U}(t,x)$.

Example 2: We consider the 3-D RDNN (1) with

$$\mathcal{D} = 0.01 I_3,\ \ \mathcal{W}_1 = \begin{bmatrix} 1+\frac{\pi}{4} & 20 & 0.001 \\ 0.1 & 1+\frac{\pi}{4} & 0.001 \\ 3 & -0.56 & -0.12 \end{bmatrix}$$
$$\mathcal{C} = I_3,\ \ \mathcal{W}_2 = \begin{bmatrix} -1.3\frac{\sqrt{2}\pi}{4} & 0.1 & -0.001 \\ 0.1 & -1.3\frac{\sqrt{2}\pi}{4} & 0.01 \\ 2 & -0.85 & 0.02 \end{bmatrix}.$$

$f_i(\vartheta_i(t,x)) = ([|\vartheta_i(t,x)+1| - |\vartheta_i(t,x)-1|]/2)(i = 1,2,3)$, $\mho = \{x| -0.5 \leq x \leq 0.5\}$, $\tau(t) = 0.9$, and $\mathcal{J}(t) = 0$. It is clear that $l_i^+ = 1$ and $l_i^- = 0$ $(i = 1,2,3)$. The attack signal is set as $\digamma_i(t_k,\bar{x}_p) = \frac{\theta}{\sqrt{2}}\sin(t_k + \bar{x}_p)$ $(i = 1,3)$, $\digamma_2(t_k,\bar{x}_p) = \frac{\theta}{\sqrt{2}}\cos(t_k + \bar{x}_p)$. The initial conditions of systems (1) and (4) are $\phi_{11}(s,x) = 1.5\Im(x)$, $\phi_{12}(s,x) = -2\Im(x)$, $\phi_{13}(s,x) = 0.5\Im(x)$, and $\phi_{21}(s,x) = 1.425\Im(x)$, $\phi_{22}(s,x) = -3\Im(x)$, and $\phi_{23}(s,x) = 0.55\Im(x)$, respectively, where $\Im(x) = \cos\pi x$.

We set $\alpha = 1.4$, $a = 2.7799$, $\epsilon = 11$, $\theta = 0.002$, $\rho = 1$, $m^* = 3$, $\tilde{h}_x = 0.02$, and $\bar{h} = \underline{h} = 0.0043$. By Theorem 2, we obtain the desired time–space SDC gain as follows:

$$\mathcal{K} = \begin{bmatrix} -25.3568 & -10.3852 & 1.9627 \\ 2.5893 & -17.2092 & -2.4012 \\ 1.8349 & -1.2973 & -19.4113 \end{bmatrix}.$$

The behavior of $\|\delta(t,x)\|$ without control input and with the TSSD controller $\mathcal{U}(t,x)$ is shown in Fig. 7. From Fig. 7(a), it can be seen that the trajectory of the error signal $\|\delta(t,x)\|$ is divergent if there is no control input. In contrast, Fig. 7(b) shows that the trajectory of $\delta(t,x)$ converges to the set $\mathfrak{S} = \{\delta(t,x) | \|\delta(t,x)\|^2 \leq 1.5413\}$. This implies that quasisynchronization of the drive-response RDNNs (1) and (4) is realized in the mean-square sense.

V. Conclusion

In this study, we studied the quasisynchronization problem for RDNNs with TSSD under deception attacks. By proposing a new inequality and an SDC mechanism subjected to deception attacks, and by selecting an appropriate LKF, we derived new quasisynchronization criteria for RDNNs. The new inequality is highly effective in the quasisynchronization problem for dynamical systems. The SDC mechanism is more applicable, as it can save network bandwidth and improve the cybersecurity of communications, and the desired SDC gain can be obtained by solving LMIs. Furthermore, we investigated the exponential synchronization of RDNNs with TSSD in the absence of deception attacks. In the end, we presented two examples to verify the usefulness of our theoretical results. In future work, state-dependent deception attacks, stochastic deception attacks, and arbitrary deception attacks will be considered for networked control systems [50], and quasisynchronization will be discussed for multiagent systems [51].

Appendix
Proof of Theorem 1

For $t \in [t_k, t_{k+1})$, the LKF for system (9) is selected as follows:

$$\mathcal{V}(t) = \sum_{i=1}^{6} \mathcal{V}_i(t) \tag{29}$$

where

$$\mathcal{V}_1(t) = \int_{\underline{\kappa}}^{\bar{\kappa}} \delta^T(t,x)\mathcal{H}\delta(t,x)dx$$

$$\mathcal{V}_2(t) = \int_{\underline{\kappa}}^{\bar{\kappa}} \int_{t-\tau(t)}^{t} e^{2\alpha(s-t)}\big[\delta^T(s,x)\mathcal{M}\delta(s,x) + g^T(\delta(s,x))\mathcal{Q}g(\delta(s,x))\big]dsdx$$

$$\mathcal{V}_3(t) = \int_{\underline{\kappa}}^{\bar{\kappa}} \frac{\partial\delta^T(t,x)}{\partial x}\mathcal{N}\mathcal{D}\frac{\partial\delta(t,x)}{\partial x}dx$$

$$\mathcal{V}_4(t) = (h_k - \sigma(t))\int_{\underline{\kappa}}^{\bar{\kappa}} \int_{t_k}^{t} e^{2\alpha(s-t)}\frac{\partial\delta^T(s,x)}{\partial s}\mathcal{P}\frac{\partial\delta(s,x)}{\partial s}dsdx$$

$$\mathcal{V}_5(t) = (h_k - \sigma(t))\int_{\underline{\kappa}}^{\bar{\kappa}} \zeta_1^T(t,x)\mathcal{R}\zeta_1(t,x)dx$$

$$\mathcal{V}_6(t) = (h_k - \sigma(t))\sigma(t)\int_{\underline{\kappa}}^{\bar{\kappa}} \zeta_2^T(t,x)\mathcal{S}\zeta_2(t,x)dx$$

with $\zeta_1(t,x) = \delta(t,x) - \delta(t_k,x)$ and $\zeta_2(t,x) = (1/t - t_k)\int_{t_k}^{t}\delta(s,x)ds$. It is noted that $\mathcal{V}_i(t)$ $(i = 4,5,6)$ vanishes before and after t_k. Thus, $\mathcal{V}(t)$ is continuous.

Calculating $\dot{\mathcal{V}}(t)$ along the trajectories of system (9) yields

$$\dot{\mathcal{V}}_1(t) = 2\int_{\underline{\kappa}}^{\bar{\kappa}} \delta^T(t,x)\mathcal{H}\frac{\partial\delta(t,x)}{\partial t}dx \tag{30}$$

$$\dot{\mathcal{V}}_2(t) \le -2\alpha\mathcal{V}_2(t) + \int_{\underline{\kappa}}^{\bar{\kappa}} \delta^T(t,x)\mathcal{M}\delta(t,x)dx - (1-\mu)e^{-2\alpha\tau}\int_{\underline{\kappa}}^{\bar{\kappa}} \delta^T(t-\tau(t),x)\mathcal{M}\delta(t-\tau(t),x)dx \tag{31}$$

$$- (1-\mu)e^{-2\alpha\tau}\int_{\underline{\kappa}}^{\bar{\kappa}} g^T(\delta(t-\tau(t),x))\mathcal{Q} \times g(\delta(t-\tau(t),x))dx + \int_{\underline{\kappa}}^{\bar{\kappa}} g^T(\delta(t,x))\mathcal{Q}g(\delta(t,x))dx \tag{32}$$

$$\dot{\mathcal{V}}_3(t) = 2\int_{\underline{\kappa}}^{\bar{\kappa}} \frac{\partial^2\delta^T(t,x)}{\partial x\partial t}\mathcal{N}\mathcal{D}\frac{\partial\delta(t,x)}{\partial x}dx \tag{33}$$

$$\dot{\mathcal{V}}_4(t) \le -e^{-2\alpha\bar{h}}\int_{\underline{\kappa}}^{\bar{\kappa}}\int_{t_k}^{t} \frac{\partial\delta^T(s,x)}{\partial s}\mathcal{P}\frac{\partial\delta(s,x)}{\partial s}dsdx + (h_k - \sigma(t))\int_{\underline{\kappa}}^{\bar{\kappa}} \frac{\partial\delta^T(t,x)}{\partial t}\mathcal{P}\frac{\partial\delta(t,x)}{\partial t}dx - 2\alpha\mathcal{V}_4(t) \tag{34}$$

$$\dot{\mathcal{V}}_5(t) = -\int_{\underline{\kappa}}^{\bar{\kappa}} \zeta_1^T(t,x)\mathcal{R}\zeta_1(t,x)dx + 2(h_k - \sigma(t))\int_{\underline{\kappa}}^{\bar{\kappa}} \zeta_1^T(t,x)\mathcal{R}\frac{\partial\delta(t,x)}{\partial t}dx \tag{35}$$

$$\dot{\mathcal{V}}_6(t) = (h_k - 2\sigma(t))\int_{\underline{\kappa}}^{\bar{\kappa}} \zeta_2^T(t,x)\mathcal{S}\zeta_2(t,x)dx + 2(h_k - \sigma(t))\int_{\underline{\kappa}}^{\bar{\kappa}} \zeta_2^T(t,x)\mathcal{S}[\delta(t,x) - \zeta_2(t,x)]dx. \tag{36}$$

Lemma 1 and (34) imply

$$-e^{-2\alpha\bar{h}}\int_{\underline{\kappa}}^{\bar{\kappa}}\int_{t_k}^{t} \frac{\partial\delta^T(s,x)}{\partial s}\mathcal{P}\frac{\partial\delta(s,x)}{\partial s}dsdx \le -\frac{e^{-2\alpha\bar{h}}}{\sigma(t)}\int_{\underline{\kappa}}^{\bar{\kappa}} \big[\zeta_1^T(t,x)\mathcal{P}\zeta_1(t,x) + 3\zeta_3^T(t,x)\mathcal{P}\zeta_3(t,x)\big]dx \tag{37}$$

where $\zeta_3(t,x) = \delta(t,x) + \delta(t_k,x) - 2\zeta_2(t,x)$.

Let $\zeta_4(t,x) = \mathrm{col}\{\delta(t,x),\ \delta(t_k,x)\}$ and $\zeta_5(t,x) = \mathrm{col}\{\delta(t,x),\ \delta(t_k,x),\ \zeta_2(t,x)\}$. For any matrices $\mathcal{Y}_1 \in \mathscr{R}^{n\times 2n}$ and $\mathcal{Y}_2 \in \mathscr{R}^{n\times 3n}$, the following inequalities hold:

$$\frac{1}{\sigma(t)}(\mathcal{P}\zeta_1(t,x) - \sigma(t)\mathcal{Y}_1\zeta_4(t,x))^T\mathcal{P}^{-1} \times (\mathcal{P}\zeta_1(t,x) - \sigma(t)\mathcal{Y}_1\zeta_4(t,x)) \ge 0 \tag{38}$$

and

$$\frac{1}{\sigma(t)}(\mathcal{P}\zeta_3(t,x) - \sigma(t)\mathcal{Y}_2\zeta_5(t,x))^T\mathcal{P}^{-1} \times (\mathcal{P}\zeta_3(t,x) - \sigma(t)\mathcal{Y}_2\zeta_5(t,x)) \ge 0 \tag{39}$$

from which, one obtains

$$-\frac{e^{-2\alpha\bar{h}}}{\sigma(t)}\int_{\underline{\kappa}}^{\bar{\kappa}} \zeta_1^T(t,x)\mathcal{P}\zeta_1(t,x)dx \le -2e^{-2\alpha\bar{h}}\int_{\underline{\kappa}}^{\bar{\kappa}} \zeta_1^T(t,x)\mathcal{Y}_1\zeta_4(t,x)dx + e^{-2\alpha\bar{h}}\sigma(t)\int_{\underline{\kappa}}^{\bar{\kappa}} \zeta_4^T(t,x)\mathcal{Y}_1^T\mathcal{P}^{-1}\mathcal{Y}_1\zeta_4(t,x)dx \tag{40}$$

and

$$-\frac{3e^{-2\alpha\bar{h}}}{\sigma(t)}\int_{\underline{\kappa}}^{\bar{\kappa}} \zeta_3^T(t,x)\mathcal{P}\zeta_3(t,x)dx \le -6e^{-2\alpha\bar{h}}\int_{\underline{\kappa}}^{\bar{\kappa}} \zeta_3^T(t,x)\mathcal{Y}_2\zeta_5(t,x)dx$$

$$+\,3e^{-2\alpha\bar{h}}\sigma(t)\int_{\underline{\kappa}}^{\bar{\kappa}}\zeta_5^T(t,x)\mathcal{Y}_2^T\mathcal{P}^{-1}\mathcal{Y}_2\zeta_5(t,x)dx. \quad (41)$$

By Assumption 1, we have for any diagonal matrices $\Gamma_i > 0 \in \mathscr{R}^{n\times n}(i=1,2)$ that

$$2\int_{\underline{\kappa}}^{\bar{\kappa}}\left(\daleth^-(t,x)\right)^T\Gamma_1\daleth^+(t,x)dx \geq 0 \quad (42)$$

$$2\int_{\underline{\kappa}}^{\bar{\kappa}}\left(\daleth_\tau^-(t,x)\right)^T\Gamma_2\daleth_\tau^+(t,x)dx \geq 0 \quad (43)$$

where $\daleth^-(t,x) = g(\delta(t,x)) - L^-\delta(t,x)$, $\daleth^+(t,x) = L^+\delta(t,x) - g(\delta(t,x))$, $\daleth_\tau^-(t,x) = g(\delta(t-\tau(t),x)) - L^-\delta(t-\tau(t),x)$, and $\daleth_\tau^+(t,x) = L^+\delta(t-\tau(t),x) - g(\delta(t-\tau(t),x))$.

It is noted that $\delta(t_k,\bar{x}_p) = \delta(t_k,x) - \int_{\bar{x}_p}^{x}[\partial\delta(t_k,\gamma)]/\partial\gamma)d\gamma$. For matrix $\mathcal{N} > 0 \in \mathscr{R}^{n\times n}$, one has from system (9) that

$$\begin{aligned}0 = 2\sum_{p=0}^{m-1}\int_{x_p}^{x_{p+1}}&\left(\frac{\partial\delta(t,x)}{\partial t}+\epsilon\delta(t,x)\right)^T\mathcal{N}\\ \times\Bigg[&-\frac{\partial\delta(t,x)}{\partial t}+\mathcal{D}\frac{\partial\delta^2(t,x)}{\partial x^2}-\mathcal{C}\delta(t,x)+\mathcal{W}_1 g(\delta(t,x))\\ &+\mathcal{W}_2 g(\delta(t-\tau(t),x))+\mathcal{K}\delta(t_k,x)\\ &-\mathcal{K}\int_{\bar{x}_p}^{x}\frac{\partial\delta(t_k,\gamma)}{\partial\gamma}d\gamma+\digamma(t_k,\bar{x}_p)\Bigg]dx. \end{aligned} \quad (44)$$

Using the Dirichlet boundary condition (5), integration by parts, and (44), we obtain

$$\begin{aligned}2\sum_{p=0}^{m-1}\int_{x_p}^{x_{p+1}}&\frac{\partial\delta^T(t,x)}{\partial t}\mathcal{N}\mathcal{D}\frac{\partial\delta^2(t,x)}{\partial x^2}dx\\ &=2\int_{\underline{\kappa}}^{\bar{\kappa}}\frac{\partial\delta^T(t,x)}{\partial t}\mathcal{N}\mathcal{D}\frac{\partial\delta^2(t,x)}{\partial x^2}dx\\ &=-2\int_{\underline{\kappa}}^{\bar{\kappa}}\frac{\partial^2\delta^T(t,x)}{\partial x\partial t}\mathcal{N}\mathcal{D}\frac{\partial\delta(t,x)}{\partial x}dx. \end{aligned} \quad (45)$$

Similarly

$$\begin{aligned}2\epsilon\sum_{p=0}^{m-1}\int_{x_p}^{x_{p+1}}&\delta^T(t,x)\mathcal{N}\mathcal{D}\frac{\partial\delta^2(t,x)}{\partial x^2}dx\\ &=2\epsilon\int_{\underline{\kappa}}^{\bar{\kappa}}\delta^T(t,x)\mathcal{N}\mathcal{D}\frac{\partial\delta^2(t,x)}{\partial x^2}dx\\ &=-2\epsilon\int_{\underline{\kappa}}^{\bar{\kappa}}\frac{\partial\delta^T(t,x)}{\partial x}\mathcal{N}\mathcal{D}\frac{\partial\delta(t,x)}{\partial x}dx. \end{aligned} \quad (46)$$

For any $\mathcal{T}_1 > 0 \in \mathscr{R}^{n\times n}$, from Lemma 2, we have

$$\begin{aligned}&-2\sum_{p=0}^{m-1}\int_{x_p}^{x_{p+1}}\Omega^T(t)\mathcal{N}\mathcal{K}\int_{\bar{x}_p}^{x}\frac{\partial\delta(t_k,\gamma)}{\partial\gamma}d\gamma dx\\ &\leq\sum_{p=0}^{m-1}\int_{x_p}^{x_{p+1}}\Omega^T(t)\mathcal{T}_1\Omega(t)dx+\sum_{p=0}^{m-1}\int_{x_p}^{x_{p+1}}\\ &\left[\left(\int_{\bar{x}_p}^{x}\frac{\partial\delta(t_k,\gamma)}{\partial\gamma}d\gamma\right)^T(\mathcal{N}\mathcal{K})^T\mathcal{T}_1^{-1}\mathcal{N}\mathcal{K}\int_{\bar{x}_p}^{x}\frac{\partial\delta(t_k,\gamma)}{\partial\gamma}d\gamma\right]dx\\ &=\int_{\underline{\kappa}}^{\bar{\kappa}}\Omega^T(t)\mathcal{T}_1\Omega(t)dx+\sum_{p=0}^{m-1}\left(\int_{x_p}^{\bar{x}_p}+\int_{\bar{x}_p}^{x_{p+1}}\right)\\ &\times\left[\left(\int_{\bar{x}_p}^{x}\frac{\partial\delta(t_k,\gamma)}{\partial\gamma}d\gamma\right)^T(\mathcal{N}\mathcal{K})^T\mathcal{T}_1^{-1}\mathcal{N}\mathcal{K}\int_{\bar{x}_p}^{x}\frac{\partial\delta(t_k,\gamma)}{\partial\gamma}d\gamma\right]dx\\ &\leq\int_{\underline{\kappa}}^{\bar{\kappa}}\Omega^T(t)\mathcal{T}_1\Omega(t)dx\\ &\quad+\frac{\tilde{h}_x^2}{\pi^2}\int_{\underline{\kappa}}^{\bar{\kappa}}\frac{\partial\delta(t_k,x)}{\partial x}(\mathcal{N}\mathcal{K})^T\mathcal{T}_1^{-1}\mathcal{N}\mathcal{K}\frac{\partial\delta(t_k,x)}{\partial x}dx \end{aligned} \quad (47)$$

where $\Omega(t) = ([\partial\delta(t,x)]/\partial t) + \epsilon\delta(t,x)$.

Similarly, for $\mathcal{T}_2 > 0 \in \mathscr{R}^{n\times n}$, we obtain that

$$\begin{aligned}2\sum_{p=0}^{m-1}\int_{x_p}^{x_{p+1}}&\Omega^T(t)\mathcal{N}\digamma(t_k,\bar{x}_p)dx\\ &\leq\int_{\underline{\kappa}}^{\bar{\kappa}}\Omega^T(t)\mathcal{T}_2\Omega(t)dx\\ &\quad+\int_{\underline{\kappa}}^{\bar{\kappa}}\digamma^T(t_k,\bar{x}_p)\mathcal{N}^T\mathcal{T}_2^{-1}\mathcal{N}\digamma\left(t_k,\bar{x}_p\right)dx. \end{aligned} \quad (48)$$

By Lemma 2, (46) implies that

$$\begin{aligned}2\alpha\mathcal{V}_3(t)-2\epsilon&\int_{\underline{\kappa}}^{\bar{\kappa}}\frac{\partial\delta^T(t,x)}{\partial x}\mathcal{N}\mathcal{D}\frac{\partial\delta(t,x)}{\partial x}dx\\ &=2(\alpha-\epsilon)\int_{\underline{\kappa}}^{\bar{\kappa}}\frac{\partial\delta^T(t,x)}{\partial x}\mathcal{N}\mathcal{D}\frac{\partial\delta(t,x)}{\partial x}dx\\ &\leq\frac{2(\alpha-\epsilon)\pi^2}{\left(\bar{\kappa}-\underline{\kappa}\right)^2}\int_{\underline{\kappa}}^{\bar{\kappa}}\delta^T(t,x)\mathcal{N}\mathcal{D}\delta(t,x)dx. \end{aligned} \quad (49)$$

Applying the Schur complement to (15), we obtain

$$\mathcal{N}^T\mathcal{T}_2^{-1}\mathcal{N} \leq \rho I_n. \quad (50)$$

Then, from (48), (50), and $\|\digamma(t_k,\bar{x}_p)\| \leq \theta$, one obtains

$$\int_{\underline{\kappa}}^{\bar{\kappa}}\digamma^T\left(t_k,\bar{x}_p\right)\mathcal{N}^T\mathcal{T}_2^{-1}\mathcal{N}\digamma\left(t_k,\bar{x}_p\right)dx \leq \rho\theta^2. \quad (51)$$

Combining (30)–(51), we obtain for $t_k \leq t < t_{k+1}$

$$\begin{aligned}&\dot{\mathcal{V}}(t)-a\sup_{-\tau\leq s\leq 0}\mathcal{V}(t+s)+2\alpha\mathcal{V}(t)\\ &\leq\int_{\underline{\kappa}}^{\bar{\kappa}}\eta^T(t,x)\Psi(1;h_k,\sigma(t))\eta(t,x)dx+\rho\theta^2\\ &\quad+\frac{\tilde{h}_x^2}{\pi^2}\int_{\underline{\kappa}}^{\bar{\kappa}}\frac{\partial\delta(t_k,x)}{\partial x}(\mathcal{N}\mathcal{K})^T\mathcal{T}_1^{-1}\mathcal{N}\mathcal{K}\frac{\partial\delta(t_k,x)}{\partial x}dx\\ &\quad-a\mathcal{V}(t_k)\\ &\leq\int_{\underline{\kappa}}^{\bar{\kappa}}\eta^T(t,x)\Psi(1;h_k,\sigma(t))\eta(t,x)dx+\rho\theta^2\\ &\quad+\frac{\tilde{h}_x^2}{\pi^2}\int_{\underline{\kappa}}^{\bar{\kappa}}\frac{\partial\delta(t_k,x)}{\partial x}(\mathcal{N}\mathcal{K})^T\mathcal{T}_1^{-1}\mathcal{N}\mathcal{K}\frac{\partial\delta(t_k,x)}{\partial x}dx\\ &\quad-a\mathcal{V}_1(t_k)-a\mathcal{V}_3(t_k)\\ &\leq\int_{\underline{\kappa}}^{\bar{\kappa}}\eta^T(t,x)\Psi^*(1;h_k,\sigma(t))\eta(t,x)dx+\rho\theta^2\\ &\quad+\int_{\underline{\kappa}}^{\bar{\kappa}}\frac{\partial\delta(t_k,x)}{\partial x}\left[-a\mathcal{N}\mathcal{D}+\frac{\tilde{h}_x^2}{\pi^2}(\mathcal{N}\mathcal{K})^T\mathcal{T}_1^{-1}\mathcal{N}\mathcal{K}\right]\frac{\partial\delta(t_k,x)}{\partial x}dx\\ &=\int_{\underline{\kappa}}^{\bar{\kappa}}\eta^T(t,x)\Bigg[\frac{\bar{h}-h_k}{\bar{h}-\underline{h}}\left(\frac{\underline{h}-\sigma(t)}{\underline{h}}\Psi^*(1;\underline{h},0)\right.\\ &\qquad\left.+\frac{\sigma(t)}{\underline{h}}\Psi^*(1;\underline{h},\underline{h})\right)+\frac{h_k-\underline{h}}{\bar{h}-\underline{h}}\left(\frac{\bar{h}-\sigma(t)}{\bar{h}}\Psi^*(1;\bar{h},0)\right. \end{aligned}$$

$$+ \frac{\sigma(t)}{\bar{h}}\Psi^*(1;\bar{h},\bar{h})\bigg)\bigg]\eta(t,x)dx + \rho\theta^2$$
$$+ \int_{\underline{\kappa}}^{\bar{\kappa}} \frac{\partial\delta(t_k,x)}{\partial x}\left[-a\mathcal{N}\mathcal{D} + \frac{\tilde{h}_x^2}{\pi^2}(\mathcal{N}\mathcal{K})^T\mathcal{T}_1^{-1}\mathcal{N}\mathcal{K}\right]\frac{\partial\delta(t_k,x)}{\partial x}dx. \quad (52)$$

Then, applying the Schur complement to (16)–(18), one obtains from (52) that

$$\dot{\mathcal{V}}(t) - a\sup_{-\tau\le s\le 0}\mathcal{V}(t+s) + 2\alpha\mathcal{V}(t) \le \rho\theta^2$$
$$t_k \le t < t_{k+1}. \quad (53)$$

Let $\tau = \min\{\underline{h}/2, d^*\}$. By Lemma 3, for $t_k \le t < t_{k+1}$, $k = 0, 1, 2, \ldots$, (53) yields

$$\mathcal{V}(t) \le e^{-2\xi(t-t_k)}\sup_{-\tau\le s\le 0}\mathcal{V}(t_k+s) + \bar{m} \quad (54)$$

which implies

$$\sup_{t_k-\tau\le s\le t_k}\mathcal{V}(s) \le \sup_{t_k-\tau\le s\le t_k}\bigg\{e^{-2\xi(s-t_{k-1})} \times \sup_{t_{k-1}-\tau\le s_1\le t_{k-1}}\mathcal{V}(s_1) + \bar{m}\bigg\}$$
$$= e^{-2\xi(t_k-t_{k-1}-\tau)}\sup_{t_{k-1}-\tau\le s_1\le t_{k-1}}\mathcal{V}(s_1) + \bar{m}. \quad (55)$$

Substituting (55) into (54) yields

$$\begin{aligned}\mathcal{V}(t) &\le e^{-2\xi(t-t_{k-1}-\tau)}\sup_{t_{k-1}-\tau\le s_1\le t_{k-1}}\mathcal{V}(s_1) + \bar{m}e^{-2\xi(t-t_k)} + \bar{m}\\
&\le e^{-2\xi(t-t_{k-2}-2\tau)}\sup_{t_{k-2}-\tau\le s_1\le t_{k-2}}\mathcal{V}(s_1) + \bar{m}e^{-2\xi(t-t_{k-1}-\tau)} + \bar{m}e^{-2\xi(t-t_k)} + \bar{m}\\
&\le \cdots\\
&\le e^{-2\xi(t-t_0-k\tau)}\sup_{t_0-\tau\le s_1\le t_0}\mathcal{V}(s_1) + \bar{m}e^{-2\xi(t-t_1-(k-1)\tau)} + \cdots + \bar{m}e^{-2\xi(t-t_{k-1}-\tau)} + \bar{m}e^{-2\xi(t-t_k)} + \bar{m}\\
&\le e^{-2\xi(t-t_0-k\tau)}\sup_{t_0-\tau\le s_1\le t_0}\mathcal{V}(s_1) + \bar{m}e^{-2\xi(k-1)(\underline{h}-\tau)} + \cdots + \bar{m}e^{-2\xi(\underline{h}-\tau)} + \bar{m} + \bar{m}\\
&\le e^{-2\xi(t-t_0-k\tau)}\sup_{t_0-\tau\le s_1\le t_0}\mathcal{V}(s_1) + \frac{\bar{m}}{1-e^{-2\xi(\underline{h}-\tau)}} + \bar{m}\\
&\le e^{-\xi(t-t_0)}\sup_{t_0-\tau\le s\le t_0}\mathcal{V}(s) + \bar{m}\left(1 + \frac{1}{1-e^{-\xi\underline{h}}}\right). \end{aligned} \quad (56)$$

As $\mathcal{H} \ge m^* I_n$, we have from (29)

$$\mathcal{V}(t) \ge m^*\|\delta(t,x)\|^2. \quad (57)$$

From (56) and (57), one has

$$\|\delta(t,x)\|^2 \le e^{-\xi(t-t_0)}\frac{\sup_{t_0-\tau\le s\le t_0}\mathcal{V}(s)}{m^*} + \frac{\bar{m}}{m^*}\left(1 + \frac{1}{1-e^{-\xi\underline{h}}}\right) \quad (58)$$

implying that the error signal $\delta(t,x)$ converges to

$$\mathfrak{S} = \left\{\delta(t,x)\,|\,\|\delta(t,x)\|^2 \le \frac{\bar{m}}{m^*}\left(1 + \frac{1}{1-e^{-\xi\underline{h}}}\right)\right\}. \quad (59)$$

Thus, by Definition 1, systems (1) and (4) are quasisynchronous in the mean-square sense.

References

[1] Z. Zhou and C. Gao, *Neural Network With Applications*. Beijing, China: Tsinghua Univ. Press, 2004.
[2] R. Saravanakumar, G. Rajchakit, C. Ahn, and H. Karimi, "Exponential stability, passivity, and dissipativity analysis of generalized neural networks with mixed time-varying delays," *IEEE Trans. Syst., Man, Cybern., Syst.*, vol. 49, no. 2, pp. 395–405, Feb. 2019.
[3] L. Wang, Z. Zeng, and M.-F. Ge, "A disturbance rejection framework for finite-time and fixed-time stabilization of delayed memristive neural networks," *IEEE Trans. Syst., Man, Cybern., Syst.*, vol. 51, no. 2, pp. 905–915, Feb. 2021.
[4] H. Shen, S. Jiao, J. Cao, and T. Huang, "An improved result on sampled-data synchronization of Markov jump delayed neural networks," *IEEE Trans. Syst., Man, Cybern., Syst.*, vol. 51, no. 6, pp. 3608–3616, Jun. 2021.
[5] X. Peng and H. Wu, "Non-fragile robust finite-time stabilization and H_∞ performance analysis for fractional-order delayed neural networks with discontinuous activations under the asynchronous switching," *Neural Comput. Appl.*, vol. 32, no. 8, pp. 4045–4071, 2020.
[6] J. H. Park, H. Shen, X. Chang, and T. Lee, *Recent Advances in Control and Filtering of Dynamic Systems with Constrained Signals*. Cham, Switzerland: Springer, 2018.
[7] L. M. Pecora and T. L. Carroll, "Synchronization in chaotic systems," *Phys. Rev. Lett.*, vol. 64, no. 8, pp. 821–824, 1990.
[8] U. Parlitz, L. O. Chua, L. Kocarev, K. S. Halle, and A. Shang, "Transmission of digital signals by chaotic synchronization," *Int. J. Bifurcation Chaos*, vol. 2, no. 4, pp. 973–977, 1992.
[9] J. Zhang, X. Zhao, and J. Huang, "Synchronization control of neural networks with state-dependent coefficient matrices," *IEEE Trans. Neural Netw. Learn. Syst.*, vol. 27, no. 11, pp. 2440–2447, Nov. 2016.
[10] W. Zhao and H. Wu, "Fixed-time synchronization of semi-Markovian jumping neural networks with time-varying delays," *Adv. Differ. Equ.*, vol. 213, pp. 1–21, Jun. 2018.
[11] J. Liu, H. Wu, and J. Cao, "Event-triggered synchronization in fixed time for semi-Markov switching dynamical complex networks with multiple weights and discontinuous nonlinearity," *Commun. Nonlinear Sci. Numer. Simulat.*, vol. 90, Nov. 2020, Art. no. 105400.
[12] Y. Li, B. Luo, D. Liu, Y. Yang, and Z. Yang, "Robust exponential synchronization for memristor neural networks with nonidentical characteristics by pinning control," *IEEE Trans. Syst., Man, Cybern., Syst.*, vol. 51, no. 3, pp. 1966–1980, Mar. 2021.
[13] Y. Sheng, H. Zhang, and Z. Zeng, "Stability and robust stability of stochastic reaction–diffusion neural networks with infinite discrete and distributed delays," *IEEE Trans. Syst., Man, Cybern., Syst.*, vol. 50, no. 5, pp. 1721–1732, May 2020.
[14] L. Shanmugam, P. Mani, R. Rajan, and Y. H. Joo, "Adaptive synchronization of reaction–diffusion neural networks and its application to secure communication," *IEEE Trans. Cybern.*, vol. 50, no. 3, pp. 911–922, Mar. 2020.
[15] J. D. Murray, *Mathematical Biology*. New York, NY, USA: Springer-Verlag, 1989.
[16] J.-L. Wang, H.-N. Wu, T. Huang, S.-Y. Ren, and J. Wu, "Passivity analysis of coupled reaction–diffusion neural networks with Dirichlet boundary conditions," *IEEE Trans. Syst., Man, Cybern., Syst.*, vol. 47, no. 8, pp. 2148–2159, Aug. 2017.
[17] A. Selivanov and E. Fridman, "Boundary observers for a reaction–diffusion system under time-delayed and sampled-data measurements," *IEEE Trans. Autom. Control*, vol. 64, no. 8, pp. 3385–3390, Aug. 2019.
[18] L. O. Chua, M. Hasler, G. S. Moschytz, and J. Neirynck, "Autonomous cellular neural networks: A unified paradigm for pattern formation and active wave propagation," *IEEE Trans. Circuits Syst. I, Fundam. Theory Appl.*, vol. 42, no. 10, pp. 559–511, Oct. 1995.
[19] P. Arena, L. Fortuna, and M. Branciforte, "Reaction–diffusion CNN algorithms to generate and control artificial locomotion," *IEEE Trans. Circuits Syst. I, Fundam. Theory Appl.*, vol. 46, no. 2, pp. 253–260, Feb. 1999.

[20] J.-L. Wang, X.-X. Zhang, H.-N. Wu, T. Huang, and Q. Wang, "Finite-time passivity and synchronization of coupled reaction–diffusion neural networks with multiple weights," *IEEE Trans. Cybern.*, vol. 49, no. 9, pp. 3385–3397, Sep. 2019.

[21] X. Song, J. Man, C. K. Ahn, and S. Song, "Finite-time dissipative synchronization for Markovian jump generalized inertial neural networks with reaction–diffusion terms," *IEEE Trans. Syst., Man, Cybern., Syst.*, vol. 51, no. 6, pp. 3650–3661, Jun. 2021.

[22] R. Zhang, D. Zeng, J. H. Park, Y. Liu, and X. Xie, "Adaptive event-triggered synchronization of reaction–diffusion neural networks," *IEEE Trans. Neural Netw. Learn. Syst.*, vol. 32, no. 8, pp. 3723–3735, Aug. 2021.

[23] D. Zeng, R. Zhang, J. H. Park, Z. Pu, and Y. Liu, "Pinning synchronization of directed coupled reaction–diffusion neural networks with sampled-data communications," *IEEE Trans. Neural Netw. Learn. Syst.*, vol. 31, no. 6, pp. 2092–2103, Jun. 2020.

[24] H. Chen, P. Shi, and C.-C. Lim, "Pinning impulsive synchronization for stochastic reaction–diffusion dynamical networks with delay," *Neural Netw.*, vol. 106, pp. 281–293, Oct. 2018.

[25] X. Yang, Q. Song, J. Cao, and J. Lu, "Synchronization of coupled Markovian reaction–diffusion neural networks with proportional delays via quantized control," *IEEE Trans. Neural Netw. Learn. Syst.*, vol. 30, no. 3, pp. 951–958, Mar. 2019.

[26] Y. Lv, C. Hu, J. Yu, H. Jiang, and T. Huang, "Edge-based fractional-order adaptive strategies for synchronization of fractional-order coupled networks with reaction–diffusion terms," *IEEE Trans. Cybern.*, vol. 50, no. 4, pp. 1582–1594, Apr. 2020.

[27] Z. Guo, S. Wang, and J. Wang, "Global exponential synchronization of coupled delayed memristive neural networks with reaction–diffusion terms via distributed pinning controls," *IEEE Trans. Neural Netw. Learn. Syst.*, vol. 32, no. 1, pp. 105–116, Jan. 2021.

[28] Y. Liu, B.-Z. Guo, J. H. Park, and S.-M. Lee, "Nonfragile exponential synchronization of delayed complex dynamical networks with memory sampled-data control," *IEEE Trans. Neural Netw. Learn. Syst.*, vol. 29, no. 1, pp. 118–128, Jan. 2018.

[29] E. Fridman, "A refined input delay approach to sampled-data control," *Automatica*, vol. 26, no. 2, pp. 421–427, Feb. 2010.

[30] T. H. Lee and J. H. Park, "Improved criteria for sampled-data synchronization of chaotic Lur'e systems using two new approaches," *Nonlinear Anal. Hybrid Syst.*, vol. 24, pp. 132–145, May 2017.

[31] H. K. Lam and F. H. F. Leung, "Sampled-data fuzzy controller for time-delay nonlinear systems: Fuzzy-model-based LMI approach," *IEEE Trans. Syst., Man, Cybern. B, Cybern.*, vol. 37, no. 3, pp. 617–629, Jun. 2007.

[32] H. K. Lam and F. H. F. Leung, "Design and stabilization of sampled-data neural-network-based control systems," *IEEE Trans. Syst., Man, Cybern. B, Cybern.*, vol. 36, no. 5, pp. 995–1005, Oct. 2006.

[33] B. Lu, H. Jiang, C. Hu, and A. Abdurahman, "Synchronization of hybrid coupled reaction–diffusion neural networks with time delays via generalized intermittent control with spacial sampled-data," *Neural Netw.*, vol. 105, pp. 75–87, Sep. 2018.

[34] R. Zhang, D. Zeng, J. H. Park, H. K. Lam, and X. Xie, "Fuzzy sampled-data control for synchronization of T-S fuzzy reaction–diffusion neural networks with additive time-varying delays," *IEEE Trans. Cybern.*, vol. 51, no. 5, pp. 2384–2397, May 2021.

[35] Z.-P. Wang, H.-N. Wu, J.-L. Wang, and H.-X. Li, "Quantized sampled-data synchronization of delayed reaction–diffusion neural networks under spatially point measurements," *IEEE Trans. Cybern.*, vol. 51, no. 12, pp. 5740–5751, Dec. 2021, doi: 10.1109/TCYB.2019.2960094.

[36] S. Chen, C.-C. Lim, P. Shi, and Z. Lu, "Synchronization control for reaction–diffusion FitzHugh–Nagumo systems with spatial sampled-data," *Automatica*, vol. 93, pp. 352–362, Jul. 2018.

[37] A.-Y. Lu and G.-H. Yang, "Input-to-state stabilizing control for cyber-physical systems with multiple transmission channels under denial of service," *IEEE Trans. Autom. Control*, vol. 63, no. 6, pp. 1813–1820, Jun. 2018.

[38] A. Teixeira, I. Shames, H. Sandberg, and K. H. Johansson, "A secure control framework for resource-limited adversaries," *Automatica*, vol. 51, pp. 135–148, Jan. 2015.

[39] M. Zhu and S. Martinez, "On the performance analysis of resilient networked control systems under replay attacks," *IEEE Trans. Autom. Control*, vol. 59, no. 3, pp. 804–808, Mar. 2014.

[40] Z. Gu, P. Shi, D. Yue, S. Yan, and X. Xie, "Memory-based continuous event-triggered control for networked T-S fuzzy systems against cyber-attacks," *IEEE Trans. Fuzzy Syst.*, vol. 29, no. 10, pp. 3118–3129, Oct. 2021, doi: 10.1109/TFUZZ.2020.3012771.

[41] S. Song, J. H. Park, B. Zhang, and X. Song, "Event-based adaptive fuzzy fixed-time secure control for nonlinear CPSs against unknown false data injection and backlash-like hysteresis," *IEEE Trans. Fuzzy Syst.*, early access, Apr. 2, 2021, doi: 10.1109/TFUZZ.2021.3070700.

[42] W. He, X. Gao, W. Zhong, and F. Qian, "Secure impulsive synchronization control of multi-agent systems under deception attacks," *Inf. Sci.*, vol. 459, pp. 354–368, Aug. 2018.

[43] Z. Tang, J. H. Park, and J. Feng, "Impulsive effects on quasi-synchronization of neural networks with parameter mismatches and time-varying delay," *IEEE Trans. Neural Netw. Learn. Syst.*, vol. 29, no. 4, pp. 908–919, Apr. 2018.

[44] E. Fridman and A. Blighovsky, "Robust sampled-data control of a class of semilinear parabolic systems," *Automatica*, vol. 48, no. 5, pp. 826–836, May 2012.

[45] O. Kosut, L. Jia, R. J. Thomas, and L. Tong, "Malicious data attacks on the smart grid," *IEEE Trans. Smart Grid*, vol. 2, no. 4, pp. 645–658, Dec. 2011.

[46] A. Seuret and F. Gouaisbaut, "Wirtinger-based integral inequality: Application to time-delay systems," *Automatica*, vol. 49, no. 9, pp. 2860–2866, Sep. 2013.

[47] G. H. Hardy, J. E. Littlewood, and G. Polya, *Inequalities*. Cambridge, U.K.: Cambridge Univ. Press, 1988.

[48] Y. Fan, X. Huang, Y. Li, J. Xia, and G. Chen, "Aperiodically intermittent control for quasi-synchronization of delayed memristive neural networks: An interval matrix and matrix measure combined method," *IEEE Trans. Syst., Man, Cybern., Syst.*, vol. 49, no. 11, pp. 2254–2265, Nov. 2019.

[49] Y. Li, K. Gu, J. Zhou, and S. Xu, "Estimating stable delay intervals with a discretized Lyapunov-Krasovskii functional formulation," *Automatica*, vol. 50, no. 6, pp. 1691–1697, Jun. 2014.

[50] C. Wu, X. Zhao, W. Xia, J. Liu, and T. Basar, "L_2-gain analysis for dynamic event-triggered networked control systems with packet losses and quantization," *Automatica*, vol. 129, Jul. 2021, Art. no. 109587.

[51] X. Wang, H. Wu, and J. Cao, "Global leader-following consensus in finite time for fractional-order multi-agent systems with discontinuous inherent dynamics subject to nonlinear growth," *Nonlinear Anal. Hybrid Syst.*, vol. 37, Aug. 2020, Art. no. 100888.

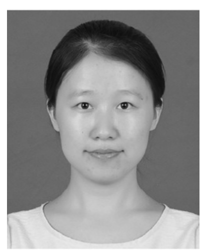

Ruimei Zhang received the Ph.D. degree in applied mathematics from the School of Mathematical Sciences, University of Electronic Science and Technology of China, Chengdu, China, in 2019.

In 2020, she joined the School of Cyber Science and Engineering, Sichuan University, Chengdu, where she is currently an Associate Researcher. From 2017 to 2018, she was a Visiting Scholar with the Department of Applied Mathematics, University of Waterloo, Waterloo, ON, Canada. From 2018 to 2019, she was a Visiting Scholar with the Department of Electrical Engineering, Yeungnam University, Gyeongsan, South Korea. Her current research interests include neural networks and networked secure control.

Hongxia Wang (Member, IEEE) received the B.S. degree from Hebei Normal University, Shijiazhuang, China, in 1996, and the M.S. and Ph.D. degrees from the University of Electronic Science and Technology of China, Chengdu, China, in 1999 and 2002, respectively.

She is a Professor with the School of Cyber Science and Engineering, Sichuan University, Chengdu. She was a Postdoctoral Researcher with Shanghai Jiao Tong University, Shanghai, China, from 2002 to 2004. She was a Professor with Southwest Jiaotong University, Chengdu, from 2004 to 2018. She has published over 200 peer research papers and wined 15 authorized patents. Her research interests include multimedia information security, digital forensics, information hiding and digital watermarking, and intelligent information processing.

Ju H. Park (Senior Member, IEEE) received the Ph.D. degree in electronics and electrical engineering from the Pohang University of Science and Technology (POSTECH), Pohang, Republic of Korea, in 1997.

From May 1997 to February 2000, he was a Research Associate with the Engineering Research Center-Automation Research Center, POSTECH. He joined Yeungnam University, Gyeongsan, Republic of Korea, in March 2000, where he is currently the Chuma Chair Professor. He is a coauthor of the monographs *Recent Advances in Control and Filtering of Dynamic Systems With Constrained Signals (New York, NY, USA: Springer-Nature, 2018)* and *Dynamic Systems With Time Delays: Stability and Control (New York, NY, USA: Springer-Nature, 2019)* and is an Editor of an edited volume *Recent Advances in Control Problems of Dynamical Systems and Networks (New York, NY, USA: Springer-Nature, 2020)*. His research interests include robust control and filtering, neural/complex networks, fuzzy systems, multiagent systems, and chaotic systems. He has published a number of articles in these areas.

Prof. Park has been a recipient of the Highly Cited Researchers Award by Clarivate Analytics (formerly, Thomson Reuters) since 2015 and listed in three fields, Engineering, Computer Sciences, and Mathematics, in 2019, 2020, and 2021. He also serves as an Editor for the *International Journal of Control, Automation and Systems*. He is also a Subject Editor/Advisory Editor/Associate Editor/Editorial Board Member of several international journals, including *IET Control Theory & Applications*, *Applied Mathematics and Computation*, *Journal of The Franklin Institute*, *Nonlinear Dynamics*, *Engineering Reports*, *Cogent Engineering*, the IEEE TRANSACTION ON FUZZY SYSTEMS, the IEEE TRANSACTION ON NEURAL NETWORKS AND LEARNING SYSTEMS, and the IEEE TRANSACTION ON CYBERNETICS. He is a Fellow of the Korean Academy of Science and Technology.

Hak-Keung Lam (Fellow, IEEE) received the B.Eng. (Hons.) and Ph.D. degrees from the Department of Electronic and Information Engineering, The Hong Kong Polytechnic University, Hong Kong, in 1995 and 2000, respectively.

In 2000 and 2005, he worked with the Department of Electronic and Information Engineering, The Hong Kong Polytechnic University as a Postdoctoral Fellow and a Research Fellow, respectively. He joined as a Lecturer with King's College London, London, U.K., in 2005, where he is currently a Reader. He is a coeditor of two edited volumes: *Control of Chaotic Nonlinear Circuits* (World Scientific, 2009) and *Computational Intelligence and Its Applications* (World Scientific, 2012), and an author/coauthor of three monographs: *Stability Analysis of Fuzzy-Model-Based Control Systems* (Springer, 2011), *Polynomial Fuzzy Model-Based Control Systems* (Springer, 2016), and *Analysis and Synthesis for Interval Type-2 Fuzzy-Model-Based Systems* (Springer, 2016). His current research interests include intelligent control, computational intelligence, and machine learning.

Dr. Lam has served as a program committee member, international advisory board member, invited session chair, and publication chair for various international conferences and a reviewer for various books, international journals, and international conferences. He is an Associate Editor of IEEE TRANSACTIONS ON FUZZY SYSTEMS, IEEE TRANSACTIONS ON CIRCUITS AND SYSTEMS—PART II: EXPRESS BRIEFS, *IET Control Theory and Applications*, *International Journal of Fuzzy Systems*, *Neurocomputing*, and *Nonlinear Dynamics*; and a guest editor and on the editorial board for a number of international journals. He was named as a Highly Cited Researcher.

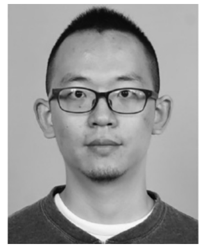

Peisong He received the B.S. degree from the University of Electronic Science and Technology of China, Chengdu, China, in 2013, and the Ph.D. degree in cybersecurity from Shanghai Jiao Tong University, Shanghai, China, in 2018.

He was working as a visiting student with the Rapid-Rich Object Search Lab, Nanyang Technological University, Singapore, from 2016 to 2017. In 2019, he joined Sichuan University, Chengdu, where he is currently an Associate Professor. His current research interest includes multimedia forensics and security.